sustainability

MDPI

Article

A Novel Hybrid MPPT Approach for Solar PV Systems Using Particle-Swarm-Optimization-Trained Machine Learning and Flying Squirrel Search Optimization

Dilip Kumar [1,*], Yogesh Kumar Chauhan [2], Ajay Shekhar Pandey [2], Ankit Kumar Srivastava [1], Varun Kumar [2], Faisal Alsaif [3], Rajvikram Madurai Elavarasan [4], Md Rabiul Islam [5], Raju Kannadasan [6] and Mohammed H. Alsharif [7,*]

1 Department of Electrical Engineering, Institute of Engineering and Technology, Dr. Rammanohar Lohia Avadh University, Ayodhya 224001, India
2 Department of Electrical Engineering, Kamla Nehru Institute of Engineering and Technology, Sultanpur 228118, India
3 Department of Electrical Engineering, College of Engineering, King Saud University, Riyadh 11421, Saudi Arabia
4 Research & Development Division (Power & Energy), Nestlives Private Limited, Chennai 600091, India
5 School of Electrical, Computer and Telecommunications Engineering, University of Wollongong, Wollongong, NSW 2522, Australia
6 Department of Electrical and Electronics Engineering, Sri Venkateswara College of Engineering, Sriperumbudur, Chennai 602117, India
7 Department of Electrical Engineering, College of Electronics and Information Engineering, Sejong University, Seoul 05006, Republic of Korea
* Correspondence: dilip1987kumar@gmail.com (D.K.); malsharif@sejong.ac.kr (M.H.A.)

Citation: Kumar, D.; Chauhan, Y.K.; Pandey, A.S.; Srivastava, A.K.; Kumar, V.; Alsaif, F.; Elavarasan, R.M.; Islam, M.R.; Kannadasan, R.; Alsharif, M.H. A Novel Hybrid MPPT Approach for Solar PV Systems Using Particle-Swarm-Optimization-Trained Machine Learning and Flying Squirrel Search Optimization. *Sustainability* **2023**, *15*, 5575. https://doi.org/10.3390/su15065575

Academic Editor: Miltiadis (Miltos) Alamaniotis

Received: 14 February 2023
Revised: 4 March 2023
Accepted: 20 March 2023
Published: 22 March 2023

Abstract: In this paper, a novel hybrid Maximum Power Point Tracking (MPPT) algorithm using Particle-Swarm-Optimization-trained machine learning and Flying Squirrel Search Optimization (PSO_ML-FSSO) has been proposed to obtain the optimal efficiency for solar PV systems. The proposed algorithm was compared with other well-known methods viz. Perturb & Observer (P&O), Incremental Conductance (INC), Particle Swarm Optimization (PSO), Cuckoo Search Optimization (CSO), Flower Pollen Algorithm (FPA), Gray Wolf Optimization (GWO), Neural-Network-trained Machine Learning (NN_ML), Genetic Algorithm (GA), and PSO-trained Machine Learning. The proposed algorithm was modelled in the MATLAB/Simulink environment under different operating conditions, for example, with step changes in temperature, solar irradiance, and partial shading. The proposed algorithm improved the efficiency up to 0.72% and reduced the settling time up to 76.4%. The findings of the research highlight that PSO_ML-FSSO is a potential approach that outperforms all other well-known algorithms tested herein for solar PV systems.

Keywords: DC–DC converter; MPPT algorithm; solar photovoltaic system

1. Introduction

It is pretty concerning how dependent the world is becoming on energy. Alternative energy sources like solar, wind, and geothermal are urgently needed given the quick degradation of traditional energy sources like coal, gas, and fossil fuels. Given that solar energy is a plentiful, endless, and clean source of energy, it can serve as a feasible alternative to produce electricity. In 2023, there will be a rise in the need for renewable energy across all industries, including heating, electricity, etc. These devices provide electricity to remote locations and places with low grid quality. In order to guarantee that the solar module always utilizes its maximum capacity, MPPT is used [1].

Traditional algorithms include P&O, INC, fractional open-circuit voltage, and fractional short circuit currents. PV systems must operate at their maximum point of power

in order to minimize expenses and improve productivity. Typically, the PV array characteristic curve ($P_{pv} \times V_{pv}$) simply displays a single MPP. However, whenever the PV array is partially shaded, this curve reveals globally and locally peak power points. As a result, most PV systems employ MPPT methods to achieve MPPs. Monitoring performance, convergence rate, as well as power fluctuations in the stable state are some performance indicators that may be used to evaluate different MPPT algorithms [2]. These methods' performances are compared using computerized simulated results (MATLAB/Simulink) for a PV system functioning in three distinct scenarios: I represents an actual test scenario with homogeneous irradiation level and II and III represent partial shadow conditions.

Under shadow conditions, panels will not generate electricity and instead they will consume a lot of energy and generate hot spots. In order to eliminate hotspots on panels, bypass diodes are linked in parallel. However, this causes many local maxima (LMs) and a single global maximum (GM) to appear on the I–V and P–V curves. The conventional MPPT algorithms include hill-climbing (HC), INC, and P&O [3]. These are undervalued because of their propensity to generate oscillations near MPPs, while being straightforward and having quick tracking capabilities. However, these approaches have a slow convergence rate and need explicit duty cycle management. Artificial Neural Networks (ANNs), GA, Machine Learning (ML), and Fuzzy Logic Controllers (FLC) with Artificial Intelligence foundations are presented in the literature. The effectiveness of these systems in monitoring the global maxima depends on the proper training of the models, which consumes a lot of computational resources and a lot of training time. Despite having a propensity to repeatedly explore the same state space, the PSO algorithm spreads knowledge via social iterations of swarm particles. The particle, however, heavily relies on co-efficient r to modify the duty cycle on a regular basis, which results in a local maximum power point (LMPP) [4]. In order to convey information, artificial bee colony (ABC) uses pheromones. Since CS uses abrupt random values, instabilities result.

A new hybrid algorithm for an MPPT approach has been presented by Hassan et al. [5] and is based on FOCV and GA. With various hybrid MPPT strategies like P&O and INC, the performance of suggested algorithm was compared. Deverakonda et al. [6] presented a hybrid model based on a neural network (NN) + P&O for PV systems and the outcomes of the proposed method were compared with the P&O method, fuzzy logic controller method (FLC), NN model, and adaptive neuro-fuzzy inference system (ANFIS) method, which are most popular MPPT algorithms. Alshareef et al. [7] discussed a new algorithm based on the falcon optimization algorithm (FOA) for the monitoring of GMPP. The proposed algorithm was evaluated on the basis of performance tracking and the result was compared with three well-known algorithms like P&O, PSO, and GWO. A new Grasshopper Optimization Algorithm (GOA) that can extract the maximum power under difficult shading conditions has been proposed by Sridhar et al. [8]. In order to eliminate the undesirable content lower-order harmonic in the cascaded H-Bridge multilevel inverter, Padmanaban et al. [9] suggested a hybrid algorithm for solar PV systems based on Artificial Neural Network-Newton Raphson (ANN-NR). Nyarco et al. [10] introduced modified variable-step-size INC method to address the issues of scale factors and step-size variation. The proposed algorithm was divided in two parts: the autonomous scaling factor and the slope change algorithm.

Castaño et al. [11] discussed the ABC-algorithm-based MPPT PV system using a DC–DC converter. To improve the power generation of PV systems dealing with changeable partial shade conditions (PSCs), Huang et al. [12] developed a unique data-driven MPPT approach. This groundbreaking work presented a GMPPT algorithm employing a P–V curve model based on natural cubic splines. A hybrid Enhanced Leader Particle Swarm Optimization (ELPSO) approach with the help of a traditional P&O strategy was used by Ram et al. [13] to discover global MPP zones. Obukhov et al. [14] introduced a new algorithm for selecting the optimal parameters of the PSO algorithm as well as parameters for the DC–DC converter to configure the solar panels. For a photovoltaic (PV) system's tracking direction and step size, Kermadi et al. [15] developed an improved MPPT algo-

rithm based on PSO and adaptive P&O. Voltage, load, and power line were combined by Li et al. [16]. A new GMPPT algorithm based on power increments was consequently developed. Ahmed et al. [17] proposed a hybrid methodology of MPPT based on enhanced adaptive perturb and observe (EA-P&O) for PV systems. By using an improved P&O method with a checking algorithm, the impact of partial shading has been calculated by Alik et al. [18] for PV systems. To find the global maximum power point, this checking algorithm compared each peak that was present on the PV curve (GMPP). In conditions of fast variation in solar irradiation and partial shadowing, Mohanty et al. [19] created a new hybrid P&O and GWO-based MPPT algorithm to extract the most power possible from a PV system PSCs. For the tracking of the MPP in both dynamic and steady state PSCs of a solar PV system, Kumar et al. [20] presented a tracking algorithm based on the whale optimization with a differential evolution (WODE) algorithm and inspired by humpback whale hunting behavior. Saibal Manna et al. [21] presented a new adaptive control framework to enhance the performance of MPPT, which will minimize the complexity in system controls and efficiently manage uncertainties and disruptions in the environment and PV system. Pradhan et al. [22] proposed a bio-inspired roach infestation optimization (RIO) algorithm to extract the maximum power from the PV system (PVS). Awan et al. [23] introduced a novel concept of data arrangement to improve the performance of the TCA in terms of MPPT speed and efficiency for solar photovoltaic (PV) systems.

Many literature reviews based on different optimization algorithms for MPPT algorithms were published in previous years (see Table 1) but to the best of the authors' knowledge, a hybrid PSO_ML-FSSO algorithm is used here for the first time for MPPT algorithms for solar PV systems. The novel contributions made in this work are:

1. A novel hybrid PSO_ML-FSSO algorithm is used for MPPT in a solar energy conversion system.
2. The performance of the algorithm is validated by comparing the results obtained from other well-known algorithms viz. P&O, INC, PSO, CSO, FPA, GWO, NN_ML, GA, and PSO_ML for different operating conditions (irradiation and temperature).

Table 1. Summary of recently published research papers for MPPT algorithm for solar PV systems.

Sr. No.	Year	Author (Ref.)	Strategies Involved	DC–DC Converter	Remarks
1.	2016	Elkholy et al. [24]	Teaching–Learning-Based Optimization (TLBO) algorithm	Boost converter	By controlling the inverter voltage and frequency, the optimal performance to obtain maximum power from PVs with minimum motor losses using TLBO algorithm was achieved.
2.	2016	Palaniswamy et al. [25]	T-S Fuzzy algorithm	Boost converter	The MPPT algorithm based on TS Fuzzy logic and INC method were developed and their efficiencies were tested.
3.	2016	Mohanty et al. [19]	Hybrid MPPT algorithm GWO and P&O	Boost converter	Developed a new GWO-P&O Hybrid-MPPT for maximum power from a PV system. The performance of the proposed method was evaluated through both simulation and experimental methods.

Table 1. *Cont.*

Sr. No.	Year	Author (Ref.)	Strategies Involved	DC–DC Converter	Remarks
4.	2017	Kumar et al. [20]	WODE-technique-based tracking algorithm	Boost converter	A hybrid algorithm based on WO and DE evolutionary techniques named WODE was proposed for MPPT under partial shading condition for PV systems.
5.	2018	Ahmed et al. [17]	The steady state oscillation and EA-P&O MPPT algorithm	Buck-Boost converter	Proposed an EA-P&O MPPT algorithm for PV systems.
6.	2018	Alik et al. [18]	Enhanced PO algorithm and a hardware implemented with Arduino Mega 2560	Boost Converter	Presented the impact of partial shading to the PV system and proposed an enhanced P&O algorithm with a checking algorithm.
7.	2018	Salam et al. [26]	The classical and proposed P&O	Boost Converter	Discussed the performance of the classical P&O method under fast-changing solar irradiation, including increase or decrease of the irradiation level with small or large steps, when the initial operating point lies to the right or left of the MPP.
8.	2018	Kermadi et al. [15]	Hybrid Adaptive P&O and PSO, SSJ Algorithm, and Incremental Conductance	Buck-boost Converter	Presented a hybrid MPPT algorithm based on adaptive P&O and PSO for PV systems.
9.	2019	Yan et al. [27]	The fixed step P&O and INC, support vector machine (SVM)	Boost converter	Proposed a novel solution to balance the trade-off between performance and cost of the MPPT algorithm.
10.	2020	Obukhov et al. [14]	PSO Algorithm	Buck converter	Presented a new algorithm for selecting the parameters of a buck converter connected to a battery.
11.	2020	Ibrahim et al. [28]	Modified PSO and ANN algorithm	Boost converter	Proposed a novel MPPT approach based on modified PSO for PV systems under PSCs
12.	2021	Sridhar et al. [8]	P&O, INC algorithms Grasshopper Optimization Algorithm (GOA)	Boost converter	A new GOA has been presented in this study.
13.	2021	Padmanaban et al. [9]	ANN-NR algorithm based Selective Harmonic Elimination (SHE) PWM, and P&O-based MPPT Algorithm	Boost converter	Introduced a hybrid ANN-NR to mitigate the undesired lower-order harmonic content in the cascaded H-Bridge multilevel inverter for solar PV systems.

Table 1. *Cont.*

Sr. No.	Year	Author (Ref.)	Strategies Involved	DC–DC Converter	Remarks
14.	2021	Castaño et al. [11]	ABC MPPT algorithm	Boost converter	Proposed the use of ABC algorithm for the MPPT of a PV system using a DC–DC converter.
15.	2022	Devarakonda et al. [6]	MPP algorithms, P&O, INC, FLC	Boost converter	Introduced a hybrid method for MPPT technique based on a neural network and P&O for PV systems.
16.	2022	Alshareef et al. [7]	FOA	Boost converter	For the monitoring of GMPP, a new strategy based on the FOA was presented in this work.
17.	2023	Kaya et al. [29]	PSO, HS, BA, ABC, FPA, DE, and CS	-	Performance of seven meta-heuristic training algorithms in the neuro-fuzzy training for MPPT.

The paper is organized as follows. The system configuration and modeling are explained in Section 2. Section 3 of the paper explains the proposed MPPT algorithm. Section 4 shows the outcomes and performance of the proposed methodology. Findings and concluding remarks are provided in Section 5.

2. System Configuration and Modeling

Equivalent Circuit Model of Solar Cell

The simplest equivalent circuit of a solar cell consists of a current source coupled in series with a diode and a variable resistor as the load is depicted in Figure 1. When the terminals are shorted together, both the output voltage as well as the voltage throughout the diode are zero [30].

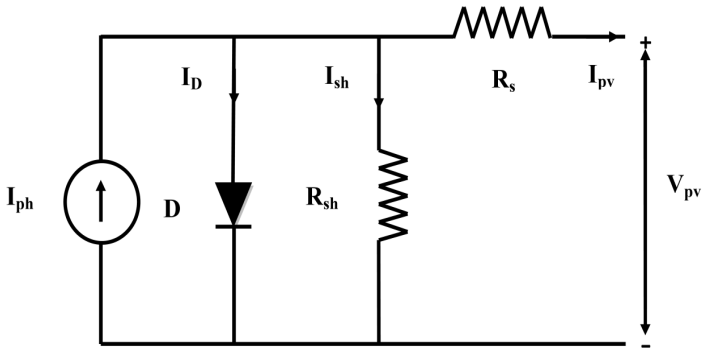

Figure 1. Equivalent circuit of solar PV system.

The output is then supplied with the total photocurrent (I_{ph}) generated by solar light. A solar cell's maximum current is (I_{sc}). When the load resistance is raised, the voltage throughout the p-n junction of the diode increases, a portion of the current passes through the diode, resulting in a corresponding decrease in output current. When the load resistor is open circuited and the whole photocurrent is flowing through the diode, the output current is zero. The diode mathematical expression can be used to calculate the relationship between current and voltage:

$$I_{pv} = I_{ph} - I_D \quad (1)$$

$$= N_p I_{SC}\left(\frac{I_r}{100}\right) - N_p I_0\left[e^{\frac{qV_{pv}}{nKTN_s}} - 1\right] \quad (2)$$

Therefore,

$$V_{pv} = \frac{N_s nKT}{q}\ln\left[\frac{N_p I_{sc}\left(\frac{I_r}{100}\right) - I_{pv}}{N_p I_o} + 1\right] \quad (3)$$

where,

I_{PV} is as the output of the current PV module;
I_0 is the diode saturating current;
I_D is the diode current;
I_{Sh} is the shunt current;
R_S is the series resistance;
R_{Sh} is the shunt resistance;
V_T is the thermal voltage;
V_{pv} is the PV array's output voltage;
I_{pv} denotes the PV array's output current;
N_S is the number of linked series cells;
N_P is the number of linked parallel cells;
K is the Boltzmann constant (whose value is $1.3806503 \times 10^{-23}$ J/K);
Q represents the electron charge (calculated value is $1.60217646 \times 10^{-19}$ C);
T is the temperature;
n is a constant and is the fill factor (ideally its value is 1).

An electric current is produced by a photoelectric effect. Once a p-n junction solar cell is lit, the intersections become forward biases, resulting in the generation of a photo-generated current, which can be represented by I_{ph} [31].

Once the load resistor gets open circuited and the whole photocurrent passes through the diode, the value of load current I_{pv} is 0. The diode's mathematical expression can be used to calculate the relationship between current and voltage

$$I_D = k_s T_c^3 exp.\left(\frac{E_g}{nkT_c}\right)(exp.\left(\frac{V_{pv} + I_{pv}R_s}{nV_t - 1}\right)) \quad (4)$$

where, k_s and n are derived by fitting parameters to the current–voltage (I–V) characteristics of the solar module, k_s is the photocurrent losses resulting from charge carrier diffusion, and n is a non-physical diode ideality factor. "E_g" is the material band gap energy (e.g., 1.12 eV for silicon) calculated from the Boltzmann's constant ($k = 1.38 \times 10^{-23}$) and the electron charge ($q = 1.6 \times 10^{-19}$), material band gap energy (1.12 eV for silicon, for example), and thermal voltage (V_t), which depends on cell temperature.

The electrical coupling of solar cells in series and/or parallel allows them to produce higher voltages, currents, and power levels.

3. Proposed Methodology

A charge controller algorithm called MPPT is used to extract the maximum power from a PV module in specific circumstances. The maximum power fluctuates with variations in irradiation from the sun, outside temperatures, and solar cell temperature. The PV cell absorbs light uniformly when there is coherent irradiance, irrespective of total radiation or total shadowing. When the sun's energy hits the PV panel in an uneven manner, partial shadowing happens [32]. The block diagram of the MPPT-based solar PV system reported in this work is depicted in Figure 2.

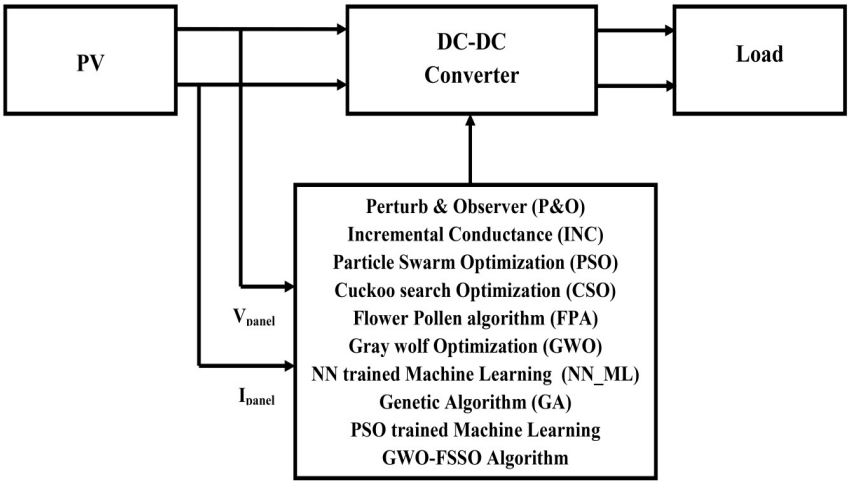

Figure 2. Block diagram of MPPT-based solar PV system.

The fundamental idea behind MPPT is to optimize the maximum amount of electricity that a PV module can produce by using the optimum effective voltage. In order to select the optimal power, which allows the PV module to deliver the maximum current into the battery, MPPT first evaluates the output of the PV module and identifies it to the battery voltage. On smoggy days or in extreme heat MPPT is utilized to extract the most power from PV modules, which frequently function better at higher temperatures. To achieve the maximum energy harvest, PV systems must therefore operate near their MPP because of the PV cell's low efficiency. In contrast to the open-circuit voltage's direct correlation with the cell temperature, the short-circuit current is only loosely correlated with solar irradiance. Hence, it is essential to have a MPPT method, which continuously monitors and analyzes the MPP to optimize the PV system's renewable power. Using MPPT depends on the region, solar field direction, season, and the time of day because photovoltaic modules receive different amounts of solar irradiation. Irradiance and temperature have similar effects on the energy utilized by each solar cell. Modelling based analysis algorithms are used to calculate V/I (voltage/current) at MPPs by employing observed voltage and current values of the PV module as raw data. Such algorithms can also be employed under uniform irradiation circumstances.

3.1. PSO-Trained Machine Learning and FSSO Hybrid

The PSO (Particle Swarm Optimization)-trained neural network is an efficient methodology for optimizing the performance of a MPPT (Maximum Power Point Tracking)-based Solar PV (Photovoltaic) system. PSO is a stochastic optimization algorithm that is inspired by the social behavior of birds in a flock, where particles (or birds) search for the best solution to a given problem by exchanging information with their neighbors in the flock. The PSO algorithm was used to train a neural network to identify the best operating point of the solar PV system, in order to maximize its power output. This is done by using the PSO algorithm to optimize the weights of the neural network, which are adjusted until the best operating point of the system is identified. The Flying Squirrel Search Optimization (FSSO) methodology is an alternative approach to identify the best operating point of the solar PV system. This method uses an iterative approach to search for the optimal operating point of the system, using a search pattern that resembles a squirrel flying in a spiral pattern. The FSSO algorithm is used to optimize the parameters of the solar PV system, such as the panel tilt angle and the panel azimuth angle, in order to maximize its power output. This method is especially useful for systems with multiple PV panels, as it allows the user to optimize the performance of the entire system, rather than just a single panel.

The PSO-trained neural network with flying squirrel search optimization (FSSO) hybrid methodology in MPPT-based solar photovoltaic (PV) systems is a technique used to optimize the maximum power point tracking (MPPT) of a solar PV system. It combines the

advantages of PSO with FSSO to improve the tracking performance of the MPPT algorithm. The PSO algorithm is used to optimize the parameters of a neural network model, which is then used to predict the maximum power of a solar PV system. This prediction is then used by the FSSO algorithm to adjust the PV system's operating point to follow the maximum power point. This hybrid methodology results in a higher efficiency in tracking the maximum power point than conventional MPPT algorithms. The advantage of using the PSO-trained neural network with FSSO hybrid methodology in MPPT-based solar PV systems is that it can quickly and accurately track the maximum power point of the PV system with less computational effort than the conventional methods. This makes it an attractive option for optimizing the performance of PV systems.

An intelligent ANN-MPPT method utilizing a MATLAB/Simulink model is proposed here. The ANN technique's output is the maximum power measurement of the PV array that is installed at the MPP, and its inputs are the weather's G level and T operations. As mentioned, how the network is trained has a significant impact on how well the ANN tool can estimate PV power. To address this technique, we developed a hybrid PSO-trained ANN with FSSO approach. The target function is also known as the mean square error. A schematic picture shows the training procedure for the PSO-trained ANN with FSSO algorithm. The flowchart of the PSO-trained ML and FSSO is shown in Figure 3.

3.2. The Best ANN System Architecture Was Determined to Be the PSO-Trained ANN Strategy

In the first stage of this update, the feed-forward ANN network's optimal topology is determined using the PSO method and the ANN model. A hybrid method was used to assess the steadily rising number of neurons in the hidden layer without requiring the user to precisely select the number, which may be incorrect. In this study, a single hidden layer of a neural network with two inputs and one output was created with the least amount of training error, and the ideal number of neurons in it was 10. This design will be used in the review to establish the appropriate initial weights for the ANN model.

3.3. Calculating the Input Weights of the ANN Model Using the PSO-Trained Method and FSSO Hybrid

The starting weights for the ANN model were enhanced. It has been demonstrated that correcting the prior beginning weight values improves the model's ability to forecast output. To accomplish this, the ANN technique was used with the PSO algorithm. The hybrid approach was used to obtain the enhanced beginning weights. The ANN model was then trained using the optimal beginning weights and the MATLAB "nntool"/"nnstart" function. The "nntool" box's field's starting weights were then switched from the enhanced initial weights to the standard training weights. The output of the ANN model optimal value training approach using real data thus achieves improved prediction compared to classical ANN. The optimized ANN model's 3D surface showed that the output power increased progressively. This approach is fairly simple to design because it does not need an additional unit during execution to guarantee completeness.

Further, the FSSO technique makes use of the flying squirrels' ability to cooperate. Furthermore, regardless of the hunter's availability, the flying squirrel position is modified [33]. The previously mentioned cooperative characteristics of flying squirrels are what led to the conversion trait. The following steps describe this strategy:

Step 1 The CFS was initially posed in the direction that was deemed to be the best option by all.
Step 2 Additionally, a portion of AS is instructed to migrate to FS in the next step.
Step 3 The remaining AS switched to CFS in the last phase.

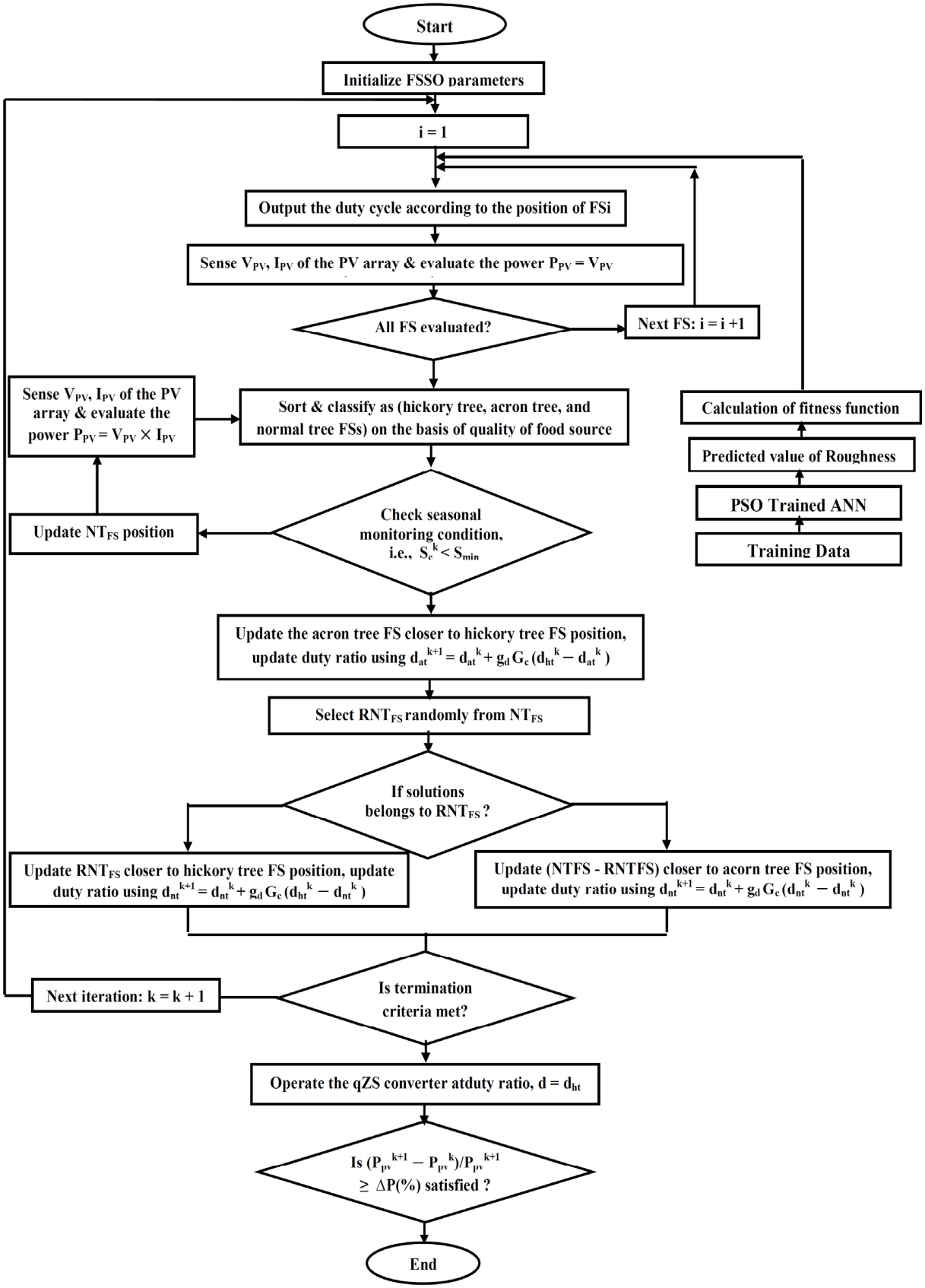

Figure 3. Flowchart of PSO_NN and FSSO hybrid algorithm.

The following assumptions are considered when using the FSSO approach for MPPT into practice:

1. The objective is analogous to the productivity of PV power in terms of the source of food supply (P_{pv}).
2. In the MPPT technique, the selection factor is viewed as a duty ratio (D) of the converter used.
3. By removing the hunter availability, the FSSO approach is appropriately customized to shorten the travel time to the GMPP.

Execution of the FSSO technique comprises several phase mechanisms.

1. Booting: Eventually, NFS FSs are positioned in the best possible locations, each of which has a specific duty ratio value for the q ZS converter, as shown below:

$$d_i = d_{mn} + \frac{(i-1)[d_{mx} - d_{mn}]}{N_{fs}}; i = 1, 2, ..., N_{fs} \tag{5}$$

where d_{mn} and d_{mx} represent the minimum and maximum duty ratios for boost operation of the converter, which equate to 10% and 90% of the permitted duty ratio, respectively.

The following is how $\frac{V_0}{V_{PV}} = \frac{1}{D_0 - D'}$ establishes the duty ratio constraints and limitations:

$$0 < d_i < 0.5$$

2. Holistic Evaluation: The converter gradually utilize search duty ratio in this procedure (i.e., the stance of each FS). A food source's description provides the instantaneous PV power yield (PPV) for each duty ratio (D). The MPPT's desired holistic expression (F), which is reproduced at each duty cycle, is written as follows:

$$\mathrm{F(D)} = \max(P_{PV}(\mathrm{D}))$$

3. Recognition and Classification: The hickory tree is deemed to have a duty cycle with a peak PV output. The acorn tree is the next best site from FS. It is expected that the remaining FS (NTFS) are situated in the typical trees.
4. Orientation upgrading: The duty cycle upgrade is communicated after examining the infrequent looking at condition. If the obligation cycles are updated using I and ($OiCO_{min}$). The state of wellbeing is then evaluated.

Random penetrating action: This technique keeps the algorithm from being stuck in neighboring maxima and preventing it from being caught. The periodic regular (OC) and its base value (O_{min}) are calculated for a single-dimensional space by:

$$O_C^i = \left| X_{at}^i - X_{ht} \right| \tag{6}$$

$$O_{min} = \frac{10e^{-6}}{365^{\frac{i}{(i_m/2.5)}}} \tag{7}$$

$$X_{ot}^{i+1} = X_{ot}^t + d \tag{8}$$

$$d = \varepsilon \frac{y \times (X_{ht} - X_{ot})}{\left| Z^{\frac{1}{\gamma}} \right|} \tag{9}$$

Action in the Trenches: The squirrel is still perched atop the hickory tree. From the acorn tree, the squirrel is travelling in the direction of the hickory tree. While the rest (NTFS RNTFS) gradually migrate away from the acorn, a few randomly selected squirrels (RNTFS) travel from normal trees and approach the hickory tree. The duty Cycle that calls for a connection are updated. In the equations that follow, it is written:

$$d_{k+1}^{at} = d_k^{at} + g_d G_c \left(d_k^{ht} - d_k^{at} \right) \tag{10}$$

$$d_{k+1}^{nt} = d_k^{nt} + g_d G_c \left(d_k^{ht} - d_k^{nt} \right) \tag{11}$$

$$d_{k+1}^{nt} = d_k^{nt} + g_d G_c \left(d_k^{at} - d_k^{nt} \right) \tag{12}$$

$$g_d = \frac{h_g}{s_f tan\varphi} \tag{13}$$

$$tan\varphi = \frac{F_D}{F_L} \tag{14}$$

$$F_D = \frac{1}{2}\rho V^2 S C_D \tag{15}$$

$$F_L = \frac{1}{2}\rho V^2 S C_L \tag{16}$$

$$\frac{P_{PV}^{k+1} - P_{PV}^{k}}{P_{PV}^{k+1}} \geq \Delta P(\%) \tag{17}$$

5. Consolidation Verification: Instead of developing into an apex, each FS's alteration illustration becomes a little dot. Additionally, the upgraded approach is ended if the allotted number of iterations has been achieved, and the duty cycle is generated at the location where the converter runs while adhering to GMPP.
6. Rebooting: When employing the MPPT, a temporal variation optimization strategy, the initial state changes regularly depending on the weather. In these circumstances, the duty ratios for FSs are restarted in order to find a brand-new GMPP.

The control parameters used in the PSO-trained neural network and flying squirrel search optimization methodology for an MPPT-based solar PV system can include:

- Maximum Power Point Tracking (MPPT) algorithm parameters such as step size, maximum and minimum voltage, and power and current limits.
- Particle swarm optimization (PSO) parameters such as population size, inertia weight, and cognitive and social parameters.
- Parameters for the neural network such as the number of neurons, learning rate, momentum, and activation functions and weights.
- Parameters for the flying squirrel search optimization methodology such as search space, population size, and mutation rate.

4. Result and Discussions

The performance investigation of the MPPT algorithms for solar PV system was carried out in MATLAB environment as shown in Figure 4. A 15 kW photovoltaic (PV) system was fitted with the PSO-trained neural network and flying squirrel optimization methodology in MPPT technology. Based on the MPPT method, a model was developed in MATLAB/Simulink to assess the efficiency of solar PV installations. A PV module, a boost converter, an MPPT controller, and a load were created as the parts of a standalone solar PV system. A solar module was used in this simulation model. Information about the solar module is provided in Table 2.

After selecting the solar panels block from the Simulink Library in the MATLAB/Simulink software 2018a, the specifications from Table 2 are inserted. The boost converter contains an inductor, an input capacitor, a MOSFET, a diode, an output capacitor, and a resistive load. It is connected to the PV block. To choose the blocks for each component, the Simulink Library was used. The MATLAB Software block for the MPPT algorithm was chosen using the Simulink Library. This block contains the integrated code for the MPPT algorithm. The PWM signal attached to the PWM generator is the block's output. The MATLAB Function block's inputs are the PV voltage and current.

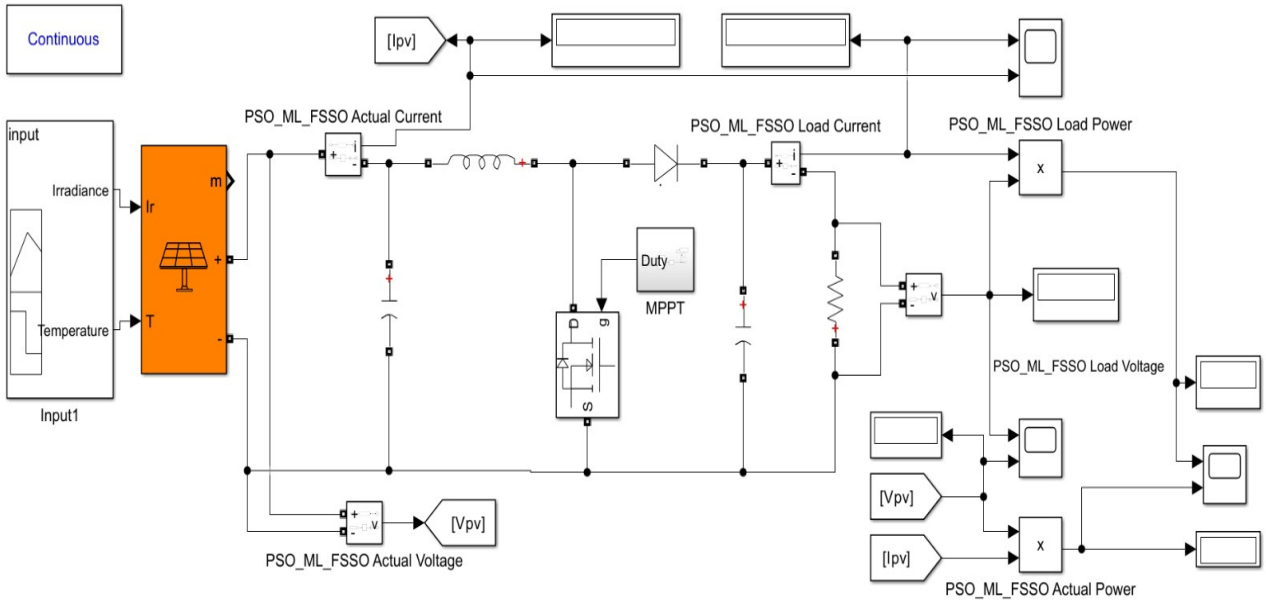

Figure 4. Simulation diagram of PV energy conversion system with various MPPT algorithms.

Table 2. System description of solar PV.

Parameter	Value
No. of PV Modules	1
Maximum Power (PMPP)	249.927
Cell Per Module (Ncell)	72
Open Circuit Voltage (VOC)	44
Short Circuit Current (ISC)	7.636
Voltage at MPP (VMPP)	36.7
Current at MPP (IMPP)	6.81
Temperature Coefficient of VOC (β)	−0.36901
Temperature Coefficient of ISC (α)	0.086998

The PWM generator is then fed the MOSFET switching device. The variation of the PWM was continuously adjusted and designed to extract the maximum power from the PV panel. Here, a DC–DC boost converter was employed to keep track of the solar PV array's maximum output. The converter has a resistive load of 2 Ω, a MOSFET power device that switches at a 20 kHz frequency with a controlled duty cycle, an inductor of 0.045875×10^{-3} H, and a capacitor of 0.259725 F.

The PV module's current and voltage readings were continuously read by the MPPT algorithms, assessed, and used to determine the duty ratio of the ensuing switching signal. The PWM signal and the Boost converter attached to the PV panel output were controlled by the operating conditions and PV attributes.

The performance of the MPPT algorithms was carried out for following cases:

1. Constant temperature (25 °C) and varying irradiation of 1000 W/m^2, 800 W/m^2, 600 W/m^2);
2. Constant irradiation (1000 W/m^2) and varying temperature (15 °C, 20 °C, and 30 °C);
3. Varying irradiation (800 W/m^2, 600 W/m^2, and 400 W/m^2) and varying temperature (35 °C, 30 °C, and 20 °C);
4. Partial shading condition.

1. Constant temperature (25 °C) and varying irradiation (1000 W/m^2, 800 W/m^2, 600 W/m^2),

The performance of the proposed novel hybrid PSO_ML-FSSO was carried out for a constant temperature (25 °C) and varying irradiation (1000 W/m^2, 800 W/m^2, and 600 W/m^2). To validate the performance, the proposed algorithm was compared with well-known MPPT algorithms viz. the P&O, INC, PSO, CSO, FPA, GWO, NN_ML, GA, and PSO_ML reported in [34–38]. The results obtained for the above cases are depicted in Figure 5. The performance of the various MPPT algorithms for constant temperature and different irradiation levels, i.e., 1000, 800, and 600 W/m^2, are summarized in Tables 3–5, respectively. From the tables, it is clear that the proposed hybrid algorithm increased the efficiency of the PV system and outperformed the other MPPT algorithms in terms of performance parameters like peak overshoot, setting time, rise time, etc. The time of tracking in PSO-trained neural networks and flying squirrel search optimization algorithm was usually faster than the other techniques. This is because the PSO technique allows the neural networks to quickly adapt to changes in the environment, resulting in faster tracking. The proposed algorithm improved the efficiency up to 0.72% and reduced the settling time up to 76.4%.

2. Constant irradiation (1000 W/m^2) and varying temperature (15 °C, 20 °C, and 30 °C)

The performance of the proposed novel hybrid PSO_ML-FSSO was then carried out for constant irradiation (1000 W/m^2) and varying temperature (15 °C, 20 °C and 30 °C). To validate the performance, the proposed algorithm was again compared with well-known MPPT algorithms viz. the P&O, INC, PSO, CSO, FPA, GWO, NN_ML, GA, and PSO_ML reported in [30–34]. The results obtained for the above cases are depicted in Figure 6. The performance of the various MPPT algorithms for constant irradiation and different temperatures i.e., 15 °C, 20 °C, and 30 °C are summarized in Tables 6–8, respectively. From the tables, it is clear that the proposed hybrid algorithm increased the efficiency of the PV system and outperformed the other MPPT algorithms in terms of performance parameters like peak overshoot, setting time, rise time, etc.

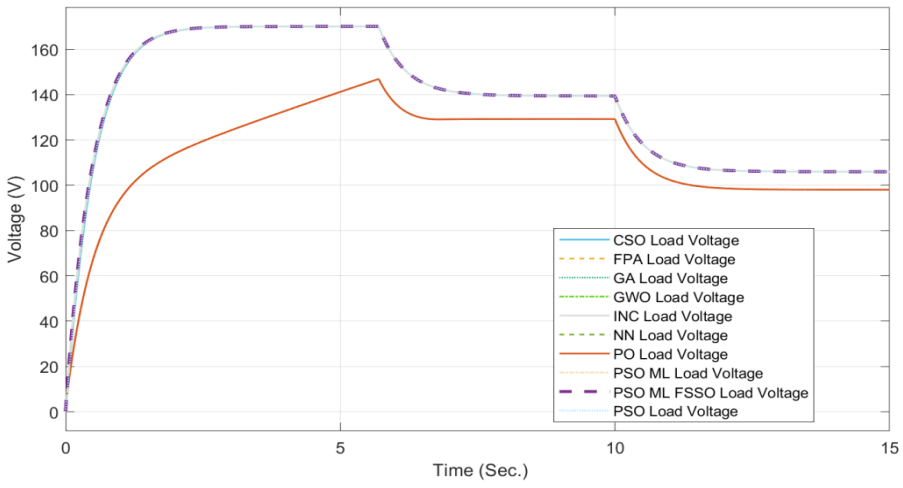

(**a**) Load Voltage

Figure 5. *Cont.*

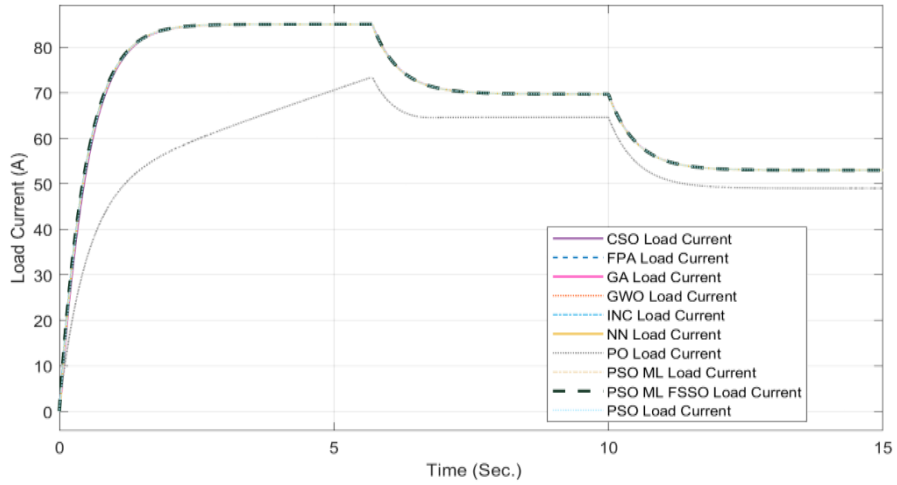

(**b**) Load Current

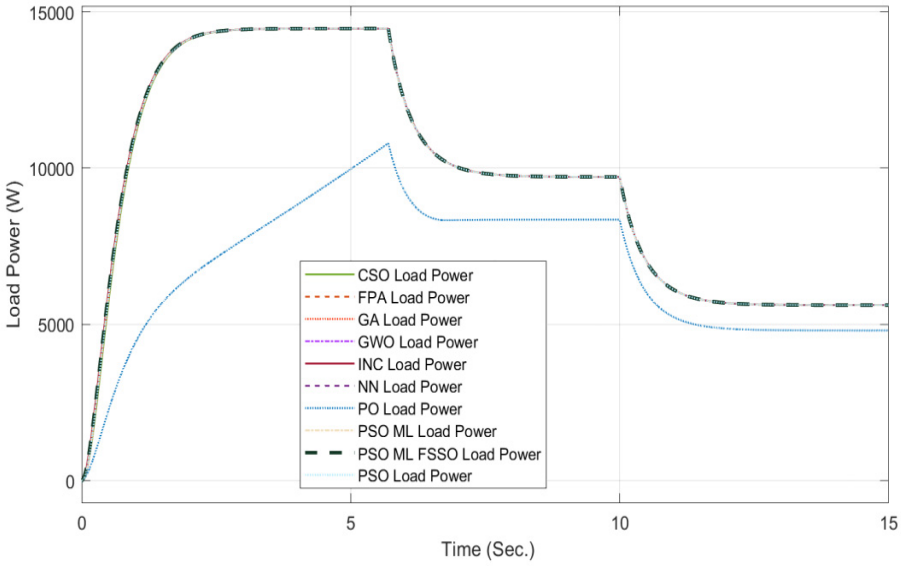

(**c**) Load Power

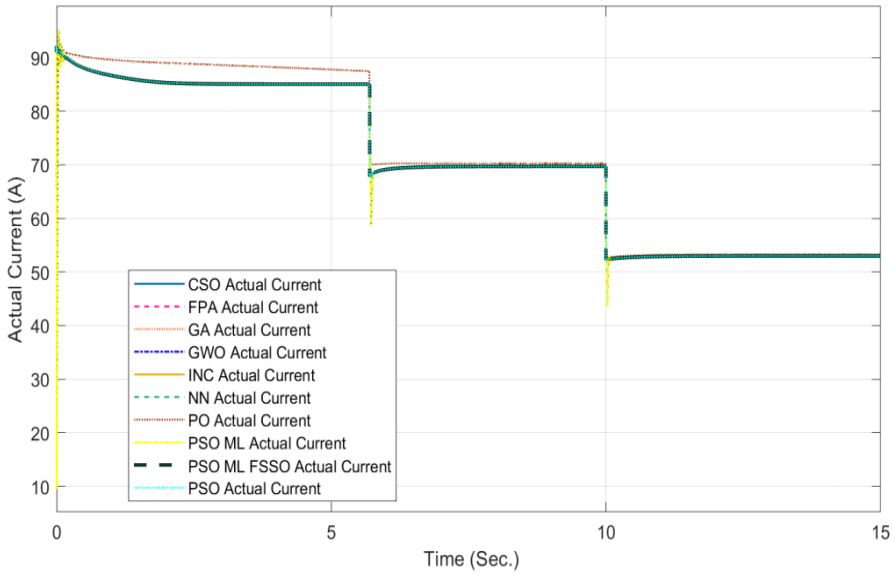

(**d**) Actual current

Figure 5. *Cont*.

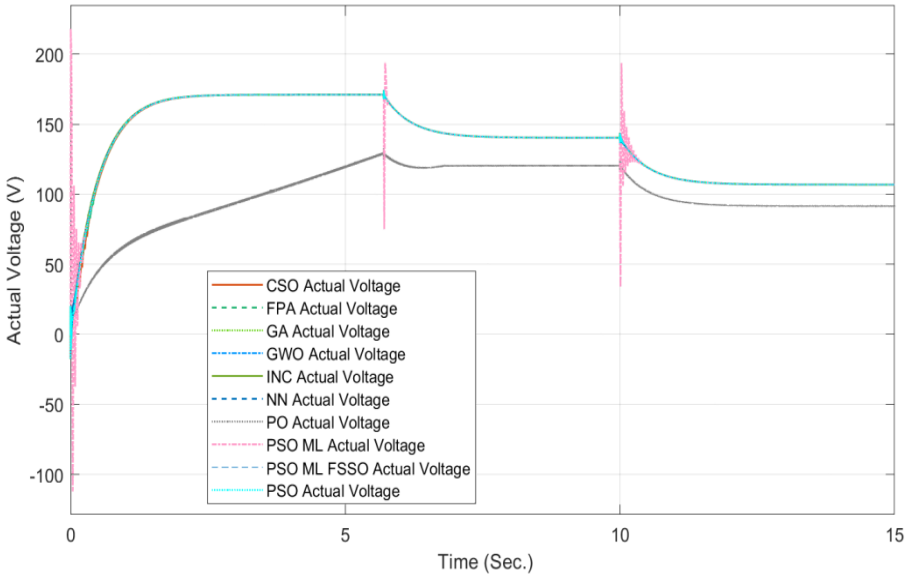

(**e**) Actual Voltage

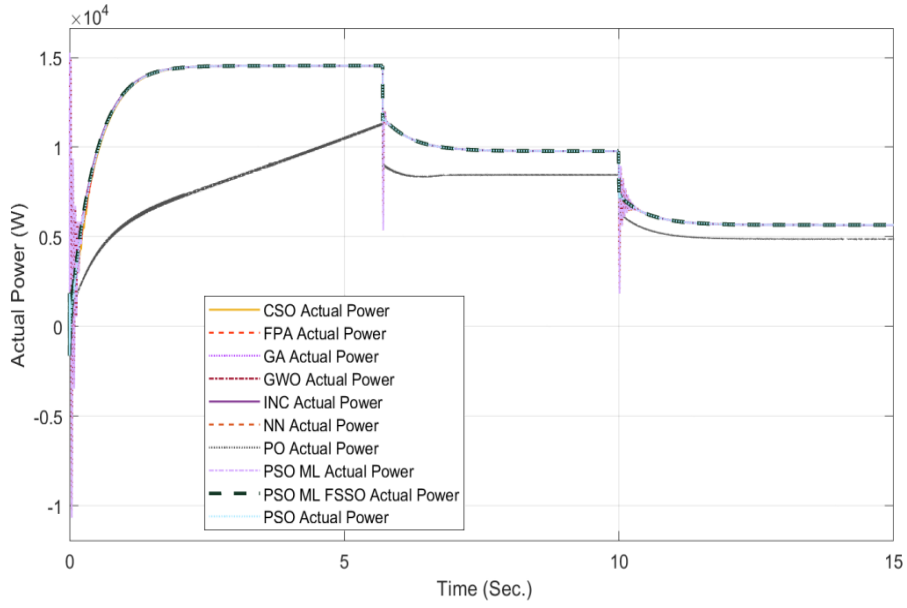

(**f**) Actual Power

Figure 5. (**a**–**f**) Results of current voltage and power at irradiance of 1000 W/m^2, 800 W/m^2, and 600 W/m^2 at constant temperature of 25 °C.

Table 3. Performance analysis of simulation results at irradiance of 1000 W/m^2 at constant temperature of 25 °C.

S. No	Algorithm	Actual Voltage (V)	Load Voltage (V)	Actual Current (A)	Load Current (A)	Actual Power (W)	Load Power (W)	Efficiency (%)	Rise Time (ms)	Settling Time (s)	Duty Cycle (%)	Overshoot (%)
1	P&O [34,35,37]	148.4	159.6	86.8	79.8	12,881.12	12,736.08	98.874	1.158	6.8	8.9	22.62
2	INC [37]	170.99	170.1	85	85	14,534.15	14,458.5	99.479	461.888	2.9	7.86	2.08
3	PSO [34]	171	170	85.05	85.05	14,543.55	14,458.55	99.415	466.014	2.05	7.90	1.92
4	CSO [34]	171	170	85.053	85	14,543.55	14,450	99.356	813.441	1.9	7.88	0.24
5	FPA [36]	171	170.11	85	85.05	14,535	14,468	99.539	461.899	1.8	7.8	2.09
6	GWO [35]	171	170.11	85	85.05	14,535	14,468	99.539	461.899	1.8	7.8	2.09
7	NN_ML [38]	171	170.15	85.05	85.056	14,543.55	14,472.3	99.510	461.888	1.9	7.76	2.08
8	GA [37]	171	170.15	85.05	85.056	14,543.55	14,472.3	99.510	461.888	1.9	7.76	2.08
9	PSO_ML [38]	171	170.15	85.05	85.056	14,543.55	14,472.3	99.510	461.888	1.9	7.76	2.08
10	PSO_ML-FSSO [Present]	171	170.25	85.06	85.098	14,545.26	14,487.3	99.601	461.888	1.6	7.63	2.08

Table 4. Performance analysis of simulation results at irradiance of 800 W/m^2 at constant temperature of 25 °C.

S. No	Algorithm	Actual Voltage (V)	Load Voltage (V)	Actual Current (A)	Load Current (A)	Actual Power (W)	Load Power (W)	Efficiency (%)	Rise Time (ms)	Settling Time (s)	Duty Cycle (%)	Overshoot (%)
1	P&O [34,35,37]	129.24	120.833	64.62	52.68	8349.55	6365.482	76.237	1.158	6.8	8.9	22.62
2	INC [37]	140.29	139.42	69.712	52.276	9779.896	7288.32	74.523	461.888	2.9	7.86	2.08
3	PSO [34]	140.295	139.421	69.713	52.277	9780.385	7288.5116	74.521	466.014	2.05	7.90	1.92
4	CSO [34]	140.296	139.425	69.713	52.2776	9780.455	7288.80	74.524	813.441	1.9	7.88	0.24
5	FPA [36]	140.299	139.426	69.714	52.279	9780.80	7289.052	74.524	461.899	1.8	7.8	2.09
6	GWO [35]	140.34	139.43	69.73	52.283	9785.91	7289.819	74.493	461.899	1.8	7.8	2.09
7	NN_ML [38]	140.54	139.48	69.743	52.289	9801.68	7301.78	74.495	461.888	1.9	7.76	2.08
8	GA [37]	140.56	139.487	69.744	52.35	9803.217	7302.14	74.487	461.888	1.9	7.76	2.08
9	PSO_ML [38]	140.61	139.52	69.756	52.42	9808.40	7313.64	74.565	461.888	1.9	7.76	2.08
10	PSO_ML-FSSO [Present]	140.61	139.72	69.857	52.62	9822.59	7352.066	74.848	461.888	1.6	7.63	2.08

Table 5. Performance analysis of simulation results at irradiance of 600 W/m^2 at constant temperature of 25 °C.

S. No	Algorithm	Actual Voltage (V)	Load Voltage (V)	Actual Current (A)	Load Current (A)	Actual Power (W)	Load Power (W)	Efficiency (%)	Rise Time (ms)	Settling Time (s)	Duty Cycle (%)	Overshoot (%)
1	P&O [34,35,37]	91.83	98.02	53.28	49.01	4892.70	4803.96	98.186	1.158	6.8	8.9	22.62
2	INC [37]	106.83	105.96	52.986	52.987	5660.494	5614.50	99.187	461.888	2.9	7.86	2.08
3	PSO [34]	106.83	105.96	52.986	52.987	5660.494	5614.50	99.187	466.014	2.05	7.90	1.92
4	CSO [34]	106.83	105.967	52.984	52.985	5660.46	5615.35	99.203	813.441	1.9	7.88	0.24
5	FPA [36]	106.831	105.98	52.987	52.988	5660.65	5615.668	99.205	461.899	1.8	7.8	2.09
6	GWO [35]	106.835	105.985	52.992	52.994	5661.4	5616.569	99.208	461.899	1.8	7.8	2.09
7	NN_ML [38]	106.94	106.115	53.004	53.050	5668.248	5629.4	99.314	461.888	1.9	7.76	2.08
8	GA [37]	106.942	106.12	53.056	53.059	5673.91	5630.62	99.237	461.888	1.9	7.76	2.08
9	PSO_ML [38]	107.11	106.27	53.23	53.28	5701.4653	5662.0656	99.308	461.888	1.9	7.76	2.08
10	PSO_ML-FSSO [Present]	107.11	106.45	53.43	53.40	5722.8873	5684.43	99.328	461.888	1.6	7.63	2.08

Table 6. Performance analysis of simulation results at temperature of 15 °C at constant irradiance of 1000 W/m^2.

S. No	Algorithm	Actual Voltage (V)	Load Voltage (V)	Actual Current (A)	Load Current (A)	Actual Power (W)	Load Power (W)	Efficiency (%)	Rise Time (ms)	Settling Time (s)	Duty Cycle (%)	Overshoot (%)
1	P&O [34,35,37]	147.885	158.3522	86.074	79.176	12,726.47	12,577.50	98.829	1.158	6.8	8.9	22.62
2	INC [37]	170.845	169.960	84.98	84.98	14,518.41	14,443.216	99.482	461.888	2.9	7.86	2.08
3	PSO [34]	170.847	169.963	84.983	84.985	14,519.09	14,443.306	99.478	466.014	2.05	7.90	1.92
4	CSO [34]	170.8458	169.9614	84.9823	84.9842	14,518.87	14,444.034	99.484	813.441	1.9	7.88	−0.24
5	FPA [36]	170.8475	169.9632	84.9842	84.9851	14,519.34	14,444.34	99.485	461.899	1.8	7.8	2.09
6	GWO [35]	170.84788	169.9633	84.9851	84.9854	14,519.524	14,444.40	99.482	461.899	1.8	7.8	2.09
7	NN_ML [38]	170.850	169.9701	84.987	84.9874	14,520.03	14,445.32	99.485	461.888	1.9	7.76	2.08
8	GA [37]	170.853	169.9709	84.9882	84.9887	14,520.49	14,445.61	99.484	461.888	1.9	7.76	2.08
9	PSO_ML [38]	170.855	169.9723	84.994	84.999	14,521.65	14,447.50	99.489	461.888	1.9	7.76	2.08
10	PSO_ML-FSSO [Present]	170.855	169.9923	85.003	85.001	14,523.18	14,449.51	99.492	461.888	1.6	7.63	2.08

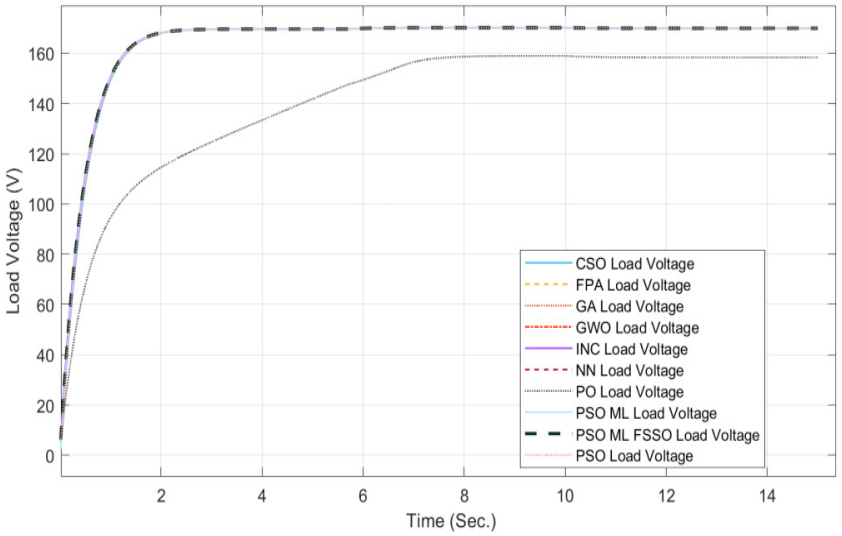

(**a**) Load Voltage

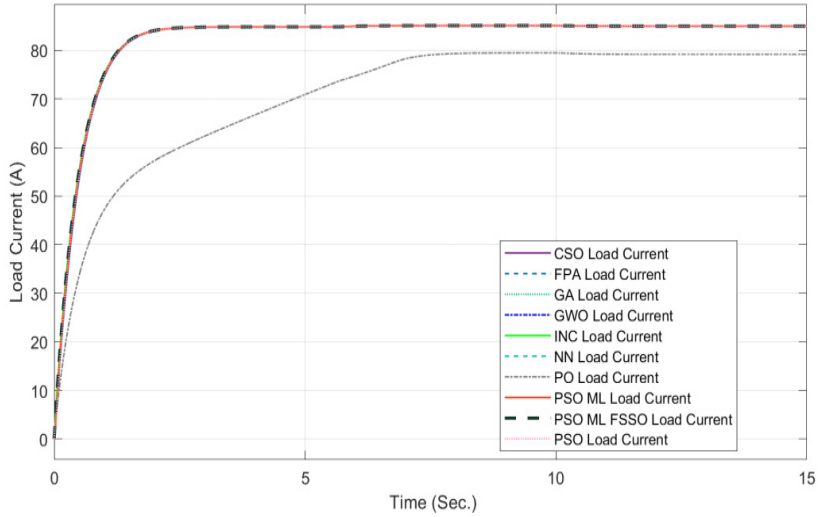

(**b**) Load Current

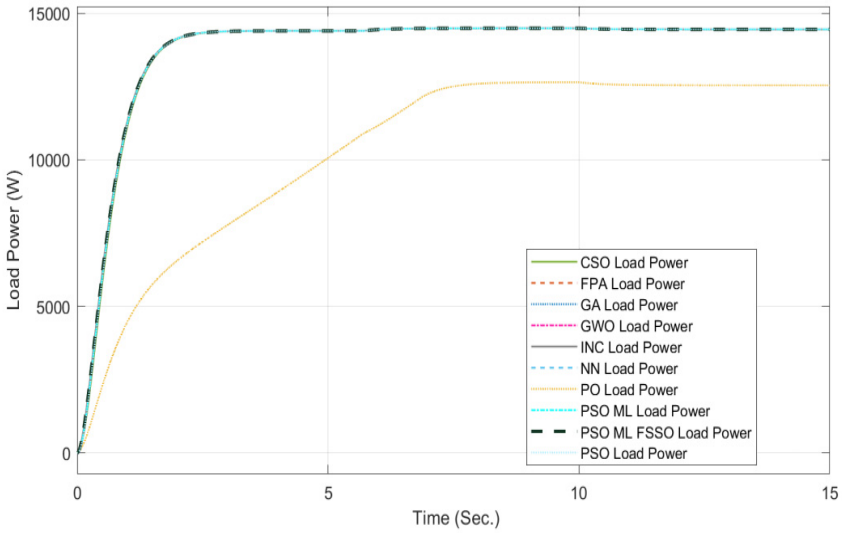

(**c**) Load Power

Figure 6. *Cont.*

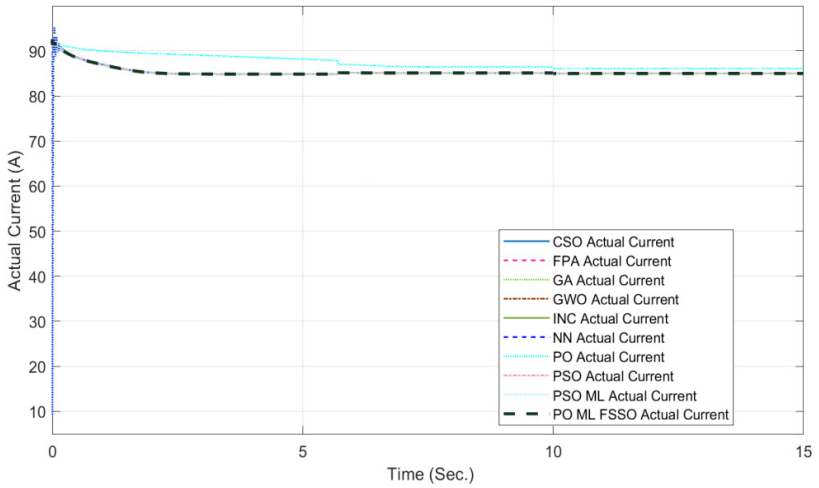

(**d**) Actual Current

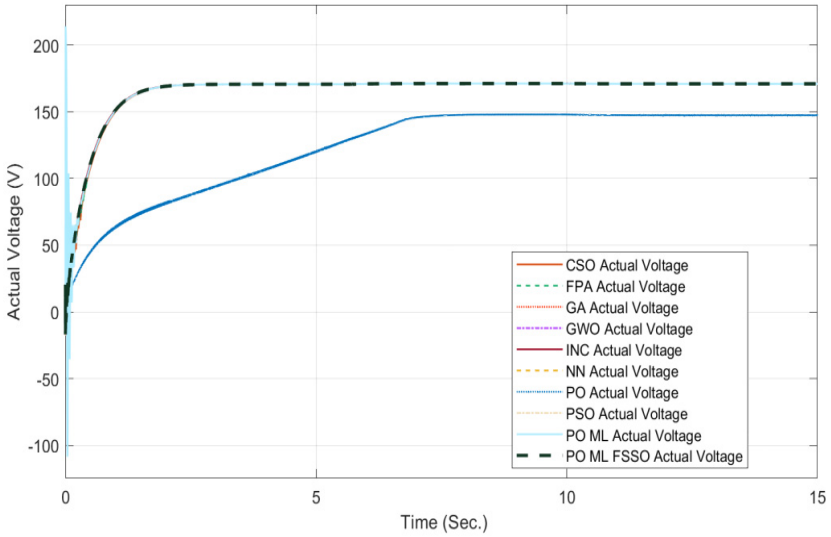

(**e**) Actual Voltage

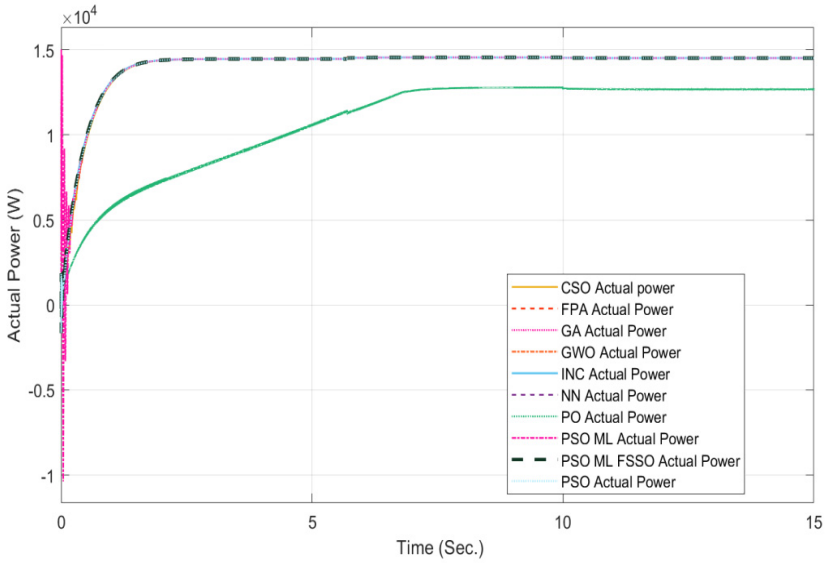

(**f**) Actual Power

Figure 6. (**a**–**f**) Results of voltage current and power at temperatures of 15 °C, 20 °C, and 30 °C at constant irradiation 1000 W/m^2.

Table 7. Performance analysis of simulation results at temperature of 20 °C at constant irradiance of 1000 W/m^2.

S. No	Algorithm	Actual Voltage (V)	Load Voltage (V)	Actual Current (A)	Load Current (A)	Actual Power (W)	Load Power (W)	Efficiency (%)	Rise Time (ms)	Settling Time (s)	Duty Cycle (%)	Overshoot (%)
1	P&O [34,35,37]	148.48	158.997	86.0516	79.498	12,777.32	12,640.11	98.926	1.158	6.8	8.9	22.62
2	INC [37]	170.181	169.066	84.96	85.090	14,458.58	14,385.83	99.496	461.888	2.9	7.86	2.08
3	PSO [34]	170.182	169.068	84.964	85.091	14,459.34	14,386.165	99.493	466.014	2.05	7.90	1.92
4	CSO [34]	170.1813	169.067	84.961	85.090	14,458.77	14,385.91	99.496	813.441	1.9	7.88	0.24%
5	FPA [36]	170.1832	169.071	84.98	85.0913	14,481.11	14,386.471	99.346	461.899	1.8	7.8	2.09
6	GWO [35]	170.1823	169.0714	84.982	85.0915	14,462.43	14,386.54	99.475	461.899	1.8	7.8	2.09
7	NN_ML [38]	170.1834	169.0723	84.991	85.0922	14,464.057	14,386.734	99.465	461.888	1.9	7.76	2.08
8	GA [37]	170.18359	169.0726	84.997	85.0925	14,481.347	14,386.81	99.347	461.888	1.9	7.76	2.08
9	PSO_ML [38]	170.18421	169.0742	84.999	85.0934	14,465.488	14,387.099	99.458	461.888	1.9	7.76	2.08
10	PSO_ML-FSSO [Present]	170.18421	169.0942	85.10	85.1905	14,482.6788	14,405.2194	99.465	461.888	1.6	7.63	2.08

Table 8. Performance analysis of simulation results at temperature of 30 °C at constant irradiance of 1000 W/m^2.

S. No	Algorithm	Actual Voltage (V)	Load Voltage (V)	Actual Current (A)	Load Current (A)	Actual Power (W)	Load Power (W)	Efficiency (%)	Rise Time (ms)	Settling Time (s)	Duty Cycle (%)	Overshoot (%)
1	P&O [34,35,37]	146.188	156.507	86.5	78.25	12,646.645	12,247.296	96.842	1.158	6.8	8.9	22.62
2	INC [37]	170.553	169.88	84.835	84.735	14,468.864	14,394.781	99.487	461.888	2.9	7.86	2.08
3	PSO [34]	170.56	169.89	84.839	84.742	14,470.14	14,396.818	99.491	466.014	2.05	7.90	1.92
4	CSO [34]	170.557	169.88	84.837	84.738	14,469.544	14,395.291	99.486	813.441	1.9	7.88	0.24
5	FPA [36]	170.563	169.92	84.841	84.742	14,470.735	14,470.360	99.506	461.899	1.8	7.8	2.09
6	GWO [35]	170.566	169.94	84.845	84.746	14,471.672	14,401.735	99.516	461.899	1.8	7.8	2.09
7	NN_ML [38]	170.602	170.007	84.851	84.752	14,475.750	14,408.433	99.534	461.888	1.9	7.76	2.08
8	GA [37]	170.606	170.012	84.853	84.7532	14,476.431	14,409.061	99.534	461.888	1.9	7.76	2.08
9	PSO_ML [38]	170.613	170.025	84.857	84.7574	14,477.71	14,410.876	99.538	461.888	1.9	7.76	2.08
10	PSO_ML-FSSO [Present]	170.613	170.025	84.868	84.7813	14,479.584	14,414.889	99.553	461.888	1.6	7.76	2.08

3. Varying irradiation (800 W/m^2, 600 W/m^2, and 400 W/m^2) and varying temperature (35 °C, 30 °C, and 20 °C)

The performance of the proposed novel hybrid PSO_ML-FSSO was then carried out for varying irradiation levels (800 W/m^2, 600 W/m^2, and 400 W/m^2) and varying temperature (35 °C, 30 °C, and 20 °C). To validate the performance, the proposed algorithm was again compared with well-known MPPT algorithms viz. the P&O, INC, PSO, CSO, FPA, GWO, NN_ML, GA, and PSO_ML reported in [34–38]. The results obtained for the above cases are depicted in Figure 7. The performance of the various MPPT algorithms for varying irradiation levels (800 W/m^2, 600 W/m^2, and 400 W/m^2) and varying temperatures of 35 °C, 30 °C, and 20 °C are summarized in Tables 9–11, respectively. From the tables, it is clear that proposed hybrid algorithm increased the efficiency of the PV system and outperformed the other MPPT algorithms in terms of performance parameters like peak overshoot, setting time, rise time, etc.

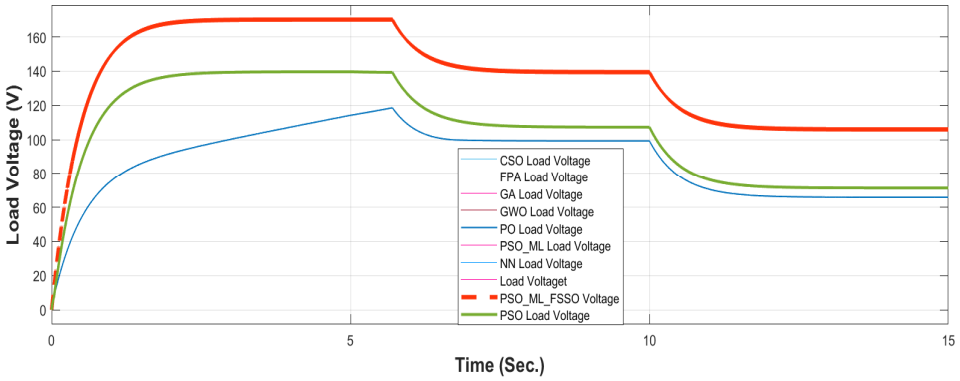

(**a**) Load Voltage

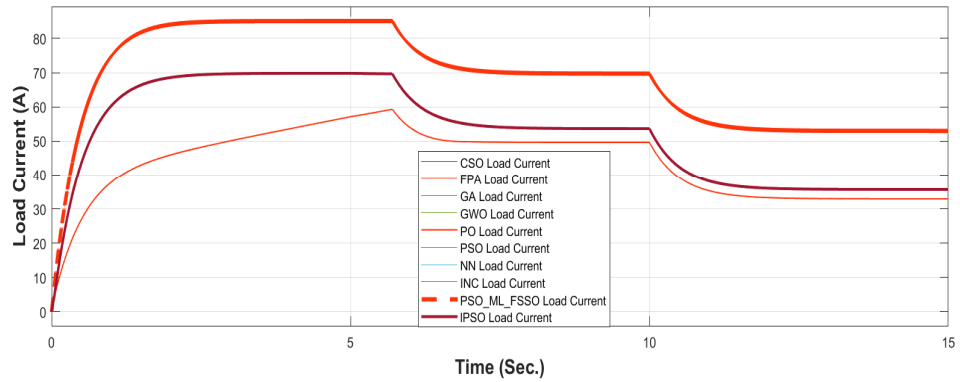

(**b**) Load Current

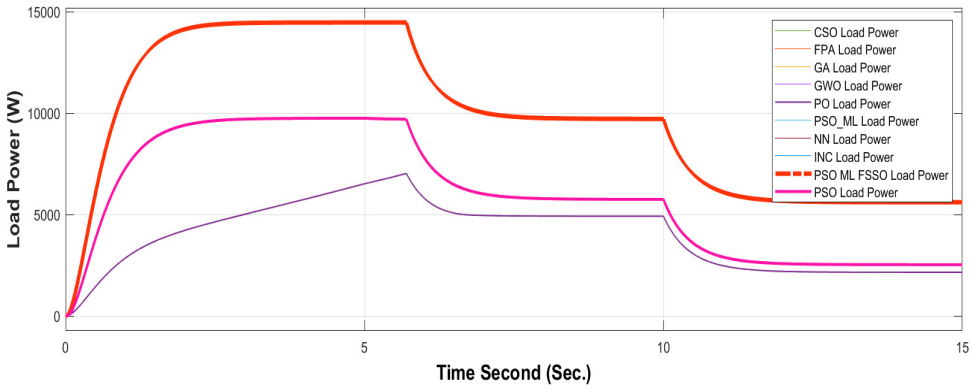

(**c**) Load Power

Figure 7. *Cont.*

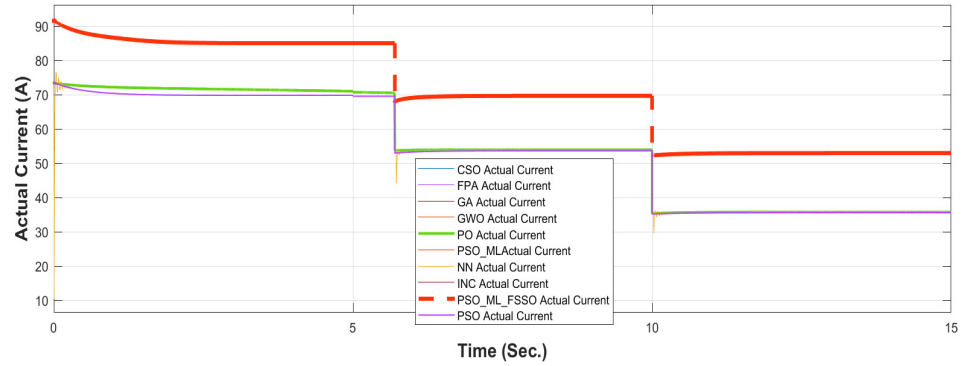

(**d**) Actual Current

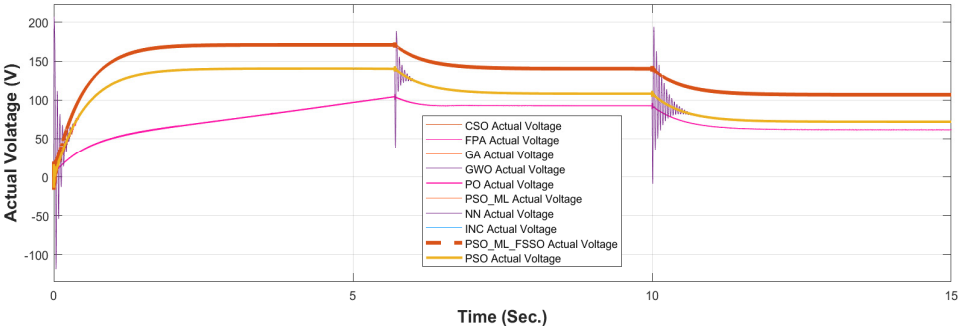

(**e**) Actual Voltage

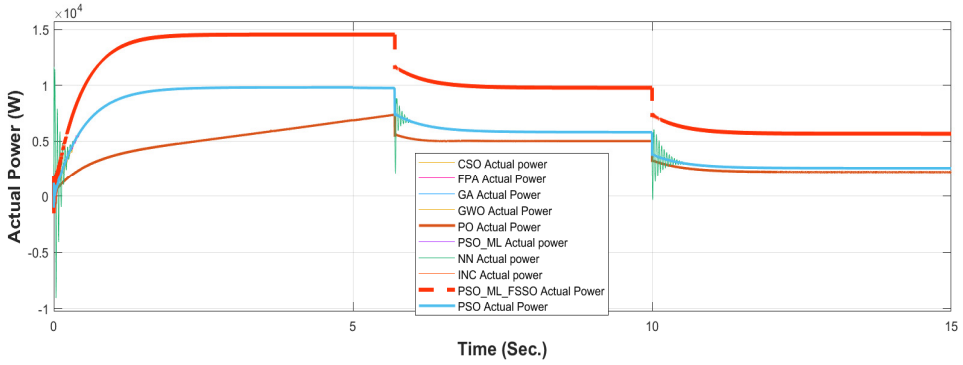

(**f**) Actual Power

Figure 7. (**a**–**f**) Results of voltage current and power at varying temperatures (35 °C, 30 °C, and 20 °C) and varying irradiation (800 W/m^2, 600 W/m^2, and 400 W/m^2).

4. Partial Shading Condition

A PV module was subject to a partial shading condition where irradiation levels are not uniform over the PV module. The model presented in this work consists of 72 cells, which are divided into three equal parts (i.e., each part consists of 24 cells) and connected in series. Three different cases were considered for a partial shading condition for the PV system for 800 W/m^2, 600 W/m^2, and 400 W/m^2 irradiation. To show the effectiveness of partial shading conditions, a comparison between a partial shading condition and without partial shading condition (i.e., 1000 W/m^2 irradiation and 25 °C temperature) was also considered in this work. The results obtained for the above cases are depicted in Figure 8. The performance of the partial shading condition for the three different cases is summarized in Table 12. From the tables, it is clear that proposed hybrid algorithm increased the efficiency of the PV system and outperformed the other MPPT algorithms in terms of performance parameters like peak overshoot, setting time, rise time, etc.

Table 9. Performance analysis of simulation results at irradiance of 800 W/m^2 at constant temperature of 35 °C.

S. No	Algorithm	Actual Voltage (V)	Load Voltage (V)	Actual Current (A)	Load Current (A)	Actual Power (W)	Load Power (W)	Efficiency (%)	Rise Time (ms)	Settling Time (s)	Duty Cycle (%)	Overshoot (%)
1	P&O [34,35,37]	111.828	110.121	56.139	55.914	6277.912	6157.305	98.078	1.158	6.8	8.9	22.62
2	INC [37]	140.519	139.649	69.830	69.824	9812.441	9750.851	99.372	461.888	2.9	7.86	2.08
3	PSO [34]	140.515	139.645	69.830	69.824	9812.162	9750.572	99.372	466.014	2.05	7.90	1.92
4	CSO [34]	140.516	139.646	69.830	69.825	9812.232	9750.781	99.373	813.441	1.9	7.88	0.24
5	FPA [36]	140.516	139.646	69.828	69.824	9811.951	9750.642	99.375	461.899	1.8	7.8	2.09
6	GWO [35]	140.519	139.649	69.830	69.824	9812.441	9750.851	99.372	461.899	1.8	7.8	2.09
7	NN_ML [38]	140.519	139.646	69.829	69.825	9812.301	9750.781	99.373	461.888	1.9	7.76	2.08
8	GA [37]	140.516	139.649	69.830	69.824	9812.232	9750.851	99.371	461.888	1.9	7.76	2.08
9	PSO_ML [38]	140.519	139.650	69.830	69.824	9812.441	9750.9216	99.373	461.888	1.9	7.76	2.08
10	PSO_ML-FSSO [Present]	185.681	184.890	77.711	77.590	14,429.477	14,345.619	99.418	461.888	1.6	7.63	2.08

Table 10. Performance analysis of simulation results at irradiance of 600 W/m^2 at constant temperature of 30 °C.

S. No	Algorithm	Actual Voltage (V)	Load Voltage (V)	Actual Current (A)	Load Current (A)	Actual Power (W)	Load Power (W)	Efficiency (%)	Rise Time (ms)	Settling Time (s)	Duty Cycle (%)	Overshoot (%)
1	P&O [34,35,37]	99.257	98.258	51.951	49.628	5156.500	4876.348	94.567	1.158	6.8	8.9	22.62
2	INC [37]	108.175	107.320	53.644	53.560	5802.939	5748.059	99.054	461.888	2.9	7.86	2.08
3	PSO [34]	108.174	107.321	53.645	53.561	5802.994	5748.220	99.056	466.014	2.05	7.90	1.92
4	CSO [34]	108.175	107.320	53.644	53.560	5802.939	5748.059	99.070	813.441	1.9	7.88	0.24
5	FPA [36]	108.174	107.319	53.646	53.560	5803.102	5748.005	99.050	461.899	1.8	7.8	2.09
6	GWO [35]	108.175	107.320	53.644	53.561	5802.939	5758.898	99.055	461.899	1.8	7.8	2.09
7	NN_ML [38]	108.174	107.321	53.644	53.560	5802.886	5748.112	99.056	461.888	1.9	7.76	2.08
8	GA [37]	108.174	107.320	53.648	53.560	5803.318	5748.059	99.047	461.888	1.9	7.76	2.08
9	PSO_ML [38]	108.173	107.320	53.644	53.561	5802.832	5748.166	99.057	461.888	1.9	7.76	2.08
10	PSO_ML-FSSO [Present]	140.709	140.158	70.066	70.056	9858.9167	9818.908	99.594	461.888	1.6	7.63	2.08

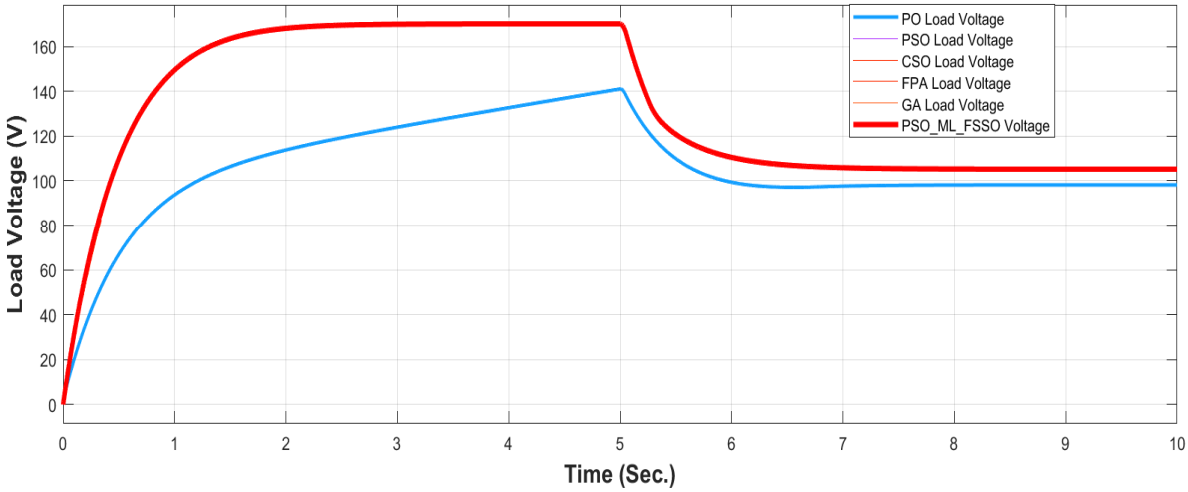

(**a**) Load Voltage

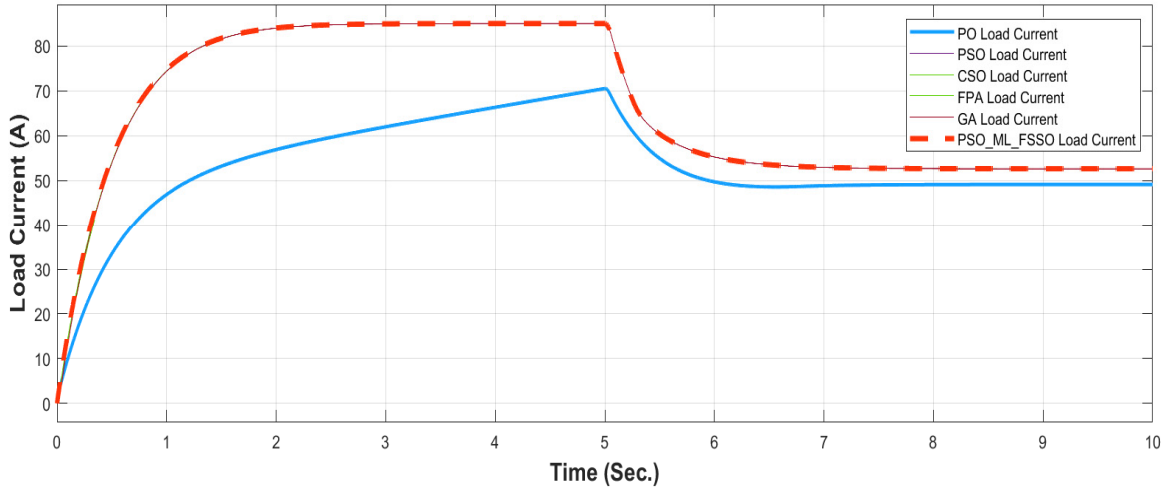

(**b**) Load Current

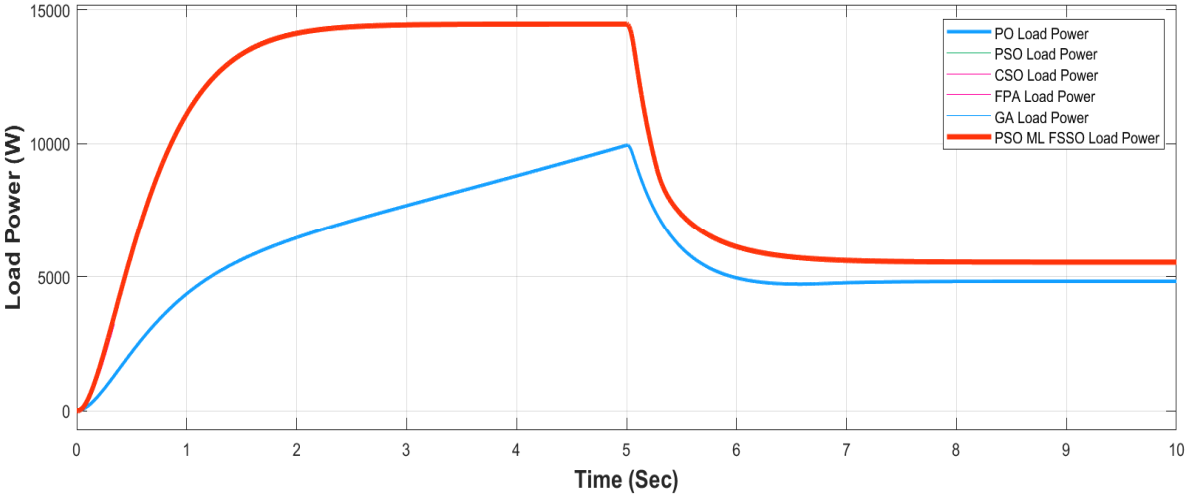

(**c**) Load Power

Figure 8. *Cont.*

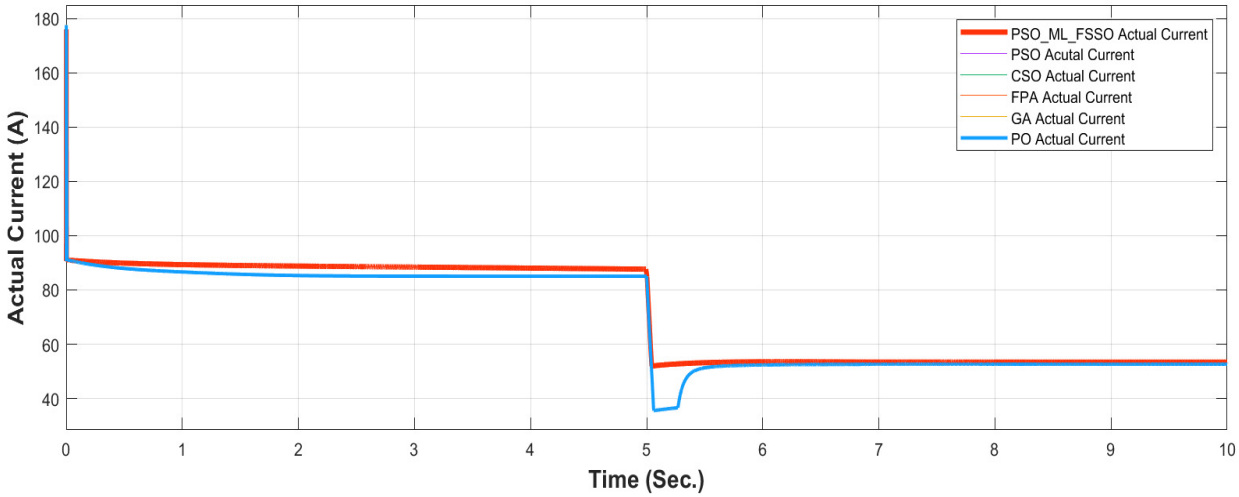

(**d**) Actual Current

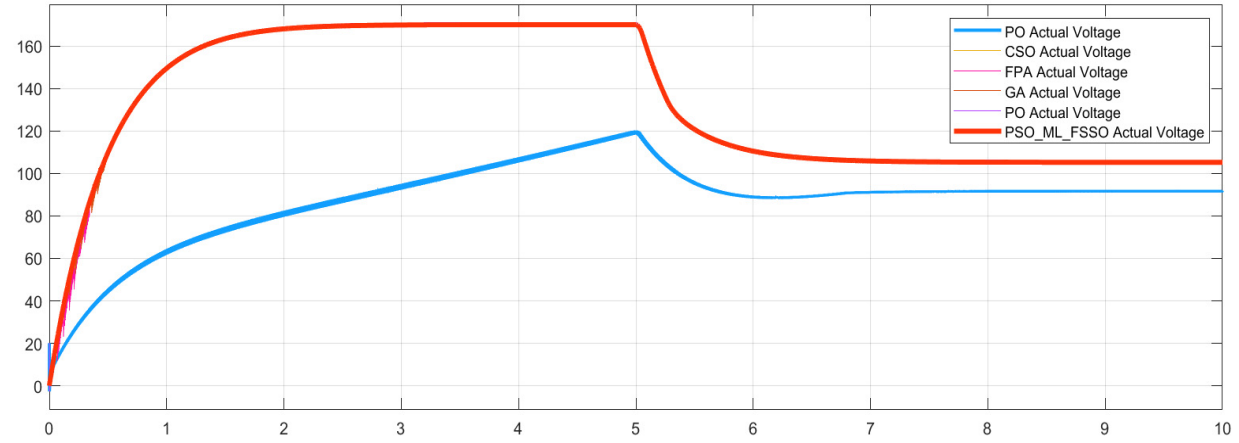

(**e**) Actual Voltage

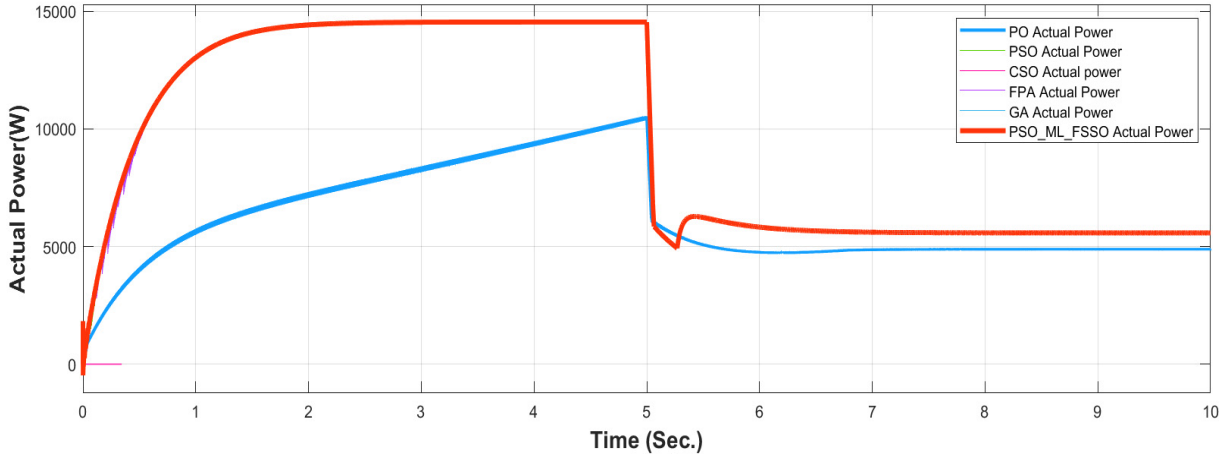

(**f**) Actual Power

Figure 8. (**a**–**f**) Results of voltage current and power in partial shading condition.

Table 11. Performance analysis of simulation results at irradiance of 400 W/m^2 at constant temperature of 20 °C.

S. No	Algorithm	Actual Voltage (V)	Load Voltage (V)	Actual Current (A)	Load Current (A)	Actual Power (W)	Load Power (W)	Efficiency (%)	Rise Time (ms)	Settling Time (s)	Duty Cycle (%)	Overshoot (%)
1	P&O [34,35,37]	67.888	65.806	35.769	32.903	2428.285	2165.214	89.166	1.158	6.8	8.9	22.62
2	INC [37]	72.109	71.273	35.635	35.027	2566.041	2496.479	97.289	461.888	2.9	7.86	2.08
3	PSO [34]	72.109	71.273	35.635	35.331	2569.604	2518.146	97.997	466.014	2.05	7.90	1.92
4	CSO [34]	72.109	71.373	35.635	35.136	2562.393	2507.762	97.868	813.441	1.9	7.88	0.24
5	FPA [36]	72.109	71.273	35.635	35.136	2573.168	2504.248	97.321	461.899	1.8	7.8	2.09
6	GWO [35]	72.109	71.173	35.635	35.436	2562.393	2522.086	98.427	461.899	1.8	7.8	2.09
7	NN_ML [38]	72.109	71.273	35.635	35.136	2573.168	2504.248	97.321	461.888	1.9	7.76	2.08
8	GA [37]	72.109	71.373	35.635	35.236	2569.604	2514.899	97.871	461.888	1.9	7.76	2.08
9	PSO_ML [38]	72.109	71.273	35.635	35.136	2569.604	2504.248	97.456	461.888	1.9	7.76	2.08
10	PSO_ML-FSSO [Present]	109.085	108.234	52.488	52.393	5725.653	5670.703	99.403	461.888	1.6	7.63	2.08

Table 12. Performance analysis of simulation results for partial shading condition.

S. No	Algorithm	Actual Voltage (V)	Load Voltage (V)	Actual Current (A)	Load Current (A)	Actual Power (W)	Load Power (W)	Efficiency (%)	Rise Time (ms)	Settling Time (s)	Duty Cycle (%)	Overshoot (%)
1	P&O [34,35,37]	91.998	98.224	53.379	49.112	4910.825	4824.030	98.232	1.158	6.8	8.9	22.62
2	INC [37]	106.083	105.230	52.619	52.615	5582.029	5536.759	99.189	461.888	2.9	7.86	2.08
3	PSO [34]	106.083	105.230	52.619	52.615	5581.592	5536.767	99.196	466.014	2.05	7.90	1.92
4	CSO [34]	106.083	105.230	52.614	52.615	5581.664	5536.769	99.195	813.441	1.9	7.88	0.24
5	FPA [36]	106.083	105.230	52.615	52.615	5581.654	5536.769	99.195	461.899	1.8	7.8	2.09
6	GWO [35]	106.083	105.230	52.669	52.615	5587.375	5536.753	99.093	461.899	1.8	7.8	2.09
7	NN_ML [38]	106.083	105.230	52.614	52.615	5581.559	5536.757	99.197	461.888	1.9	7.76	2.08
8	GA [37]	106.086	105.228	52.613	52.614	5581.308	5536.550	99.198	461.888	1.9	7.76	2.08
9	PSO_ML [38]	106.083	105.230	52.614	52.615	5581.559	5536.757	99.197	461.888	1.9	7.76	2.08
10	PSO_ML-FSSO [Present]	106.983	106.410	53.104	53.050	5681.229	5645.156	99.365	461.888	1.6	7.63	2.08

5. Conclusions

A novel hybrid MPPT algorithm based on PSO_ML-FSSO for solar PV systems has been discussed. The optimal efficiency of the proposed algorithm for PV system was achieved for four different cases. The first case was for a constant temperature and varying irradiation levels, the second case was for a constant irradiation and varying temperatures, the third case for varying irradiation levels and varying temperatures, and the last case was for a partial shading condition. The validation of the proposed algorithm was carried out by comparing the results with those obtained from other well-known MPPT algorithms viz. P&O, INC, PSO, CSO, FPA, GWO, NN_ML, GA, and PSO_ML. The results from the proposed algorithm improved the efficiency up to 0.72% and reduced the settling time up to 76.4%. The results obtained from all four cases showed the superiority of the proposed novel hybrid algorithm over the other MPPT algorithms.

Author Contributions: Conceptualization, D.K., Y.K.C. and A.S.P.; methodology, D.K., Y.K.C. and A.S.P.; software, D.K., A.K.S. and V.K.; validation, D.K., Y.K.C. and A.S.P.; formal analysis, D.K. and A.K.S.; investigation, D.K., Y.K.C. and A.S.P.; writing—original draft preparation, D.K. and A.K.S.; writing—review and editing, D.K., A.S.P., Y.K.C., R.M.E., F.A., M.R.I., R.K. and M.H.A. All authors have read and agreed to the published version of the manuscript.

Funding: This research received no external funding.

Institutional Review Board Statement: Not applicable.

Informed Consent Statement: Not applicable.

Data Availability Statement: Not applicable.

Acknowledgments: This work was supported by the Researchers Supporting Project (RSPD2023R646), King Saud University, Riyadh, Saudi Arabia.

Conflicts of Interest: The authors declare that there are no conflict of interest.

Abbreviations

ANFIS	Adaptive neuro-fuzzy inference system
ABC	Artificial bee colony
ANN-NR	Artificial Neural Network-Newton Raphson
ANN	Artificial Neural Network
CSO	Cuckoo Search Optimization
DS	Duty cycles
EA-P&O	Enhanced adaptive perturb and observe
ELPSO	Enhanced Leader Particle Swarm Optimization
FOA	Falcon optimization algorithm
FPA	Flower Pollen Algorithm
FLC	Fuzzy Logic Controllers
GA	Genetic Algorithm
GM	Global maximum
GOA	Grasshopper Optimization Algorithm
GWO	Gray Wolf Optimization
HC	Hill-climbing
INC	Incremental Conductance
LM	Local maxima
ML	Machine learning
MPPT	Maximum Power Point Tracking

NN_ML	Neural-Network-trained Machine Learning
PSCs	Partial shade conditions
PSO	Particle swarm optimization
P&O	Perturb & Observer
PV	Photovoltaic
PSO_NN	PSO-trained Machine Learning
PSO_ML-FSSO	PSO-trained Machine Learning and Flying Squirrel Search Optimization
SHE	Selective harmonic elimination
SAINCA	Self-adaptive incremental conductance algorithm
SVM	Support vector machine
TLBO	Teaching–Learning-Based Optimization
WODE	Whale optimization with differential evolution

References

1. Mendez, E.; Ortiz, A.; Ponce, P.; Macias, I.; Balderas, D.; Molina, A. Improved MPPT algorithm for photovoltaic systems based on the earthquake optimization algorithm. *Energies* **2020**, *13*, 3047. [CrossRef]
2. Oufettoul, H.; Aniba, G.; Motahhir, S. MPPT techniques investigation in photovoltaic system. In Proceedings of the 2021 9th International Renewable and Sustainable Energy Conference (IRSEC), Morocco, 23–27 November 2021; pp. 1–7.
3. Lian, K.L.; Jhang, J.H.; Tian, I.S. A maximum power point tracking method based on perturb-and-observe combined with particle swarm optimization. *IEEE J. Photovolt.* **2014**, *4*, 626–633. [CrossRef]
4. Verma, P.; Alam, A.; Sarwar, A.; Tariq, M.; Vahedi, H.; Gupta, D.; Shah Noor Mohamed, A. Meta-heuristic optimization techniques used for maximum power point tracking in solar pv system. *Electronics* **2021**, *10*, 2419. [CrossRef]
5. Hassan, A.; Bass, O.; Masoum, M.A. An improved genetic algorithm based fractional open circuit voltage MPPT for solar PV systems. *Energy Rep.* **2023**, *9*, 1535–1548. [CrossRef]
6. Devarakonda, A.K.; Karuppiah, N.; Selvaraj, T.; Balachandran, P.K.; Shanmugasundaram, R.; Senjyu, T. A comparative analysis of maximum power point techniques for solar photovoltaic systems. *Energies* **2022**, *15*, 8776. [CrossRef]
7. Alshareef, M.J. An Effective Falcon Optimization Algorithm Based MPPT Under Partial Shaded Photovoltaic Systems. *IEEE Access* **2022**, *10*, 131345–131360. [CrossRef]
8. Sridhar, R.; Subramani, C.; Pathy, S. A grasshopper optimization algorithm aided maximum power point tracking for partially shaded photovoltaic systems. *Comput. Electr. Eng.* **2021**, *92*, 107124. [CrossRef]
9. Padmanaban, S.; Dhanamjayulu, C.; Khan, B. Artificial neural network and Newton Raphson (ANN-NR) algorithm based selective harmonic elimination in cascaded multilevel inverter for PV applications. *IEEE Access* **2021**, *9*, 75058–75070. [CrossRef]
10. Owusu-Nyarko, I.; Elgenedy, M.A.; Abdelsalam, I.; Ahmed, K.H. Modified variable step-size incremental conductance MPPT technique for photovoltaic systems. *Electronics* **2021**, *10*, 2331. [CrossRef]
11. González-Castaño, C.; Restrepo, C.; Kouro, S.; Rodriguez, J. MPPT algorithm based on artificial bee colony for PV system. *IEEE Access* **2021**, *9*, 43121–43133. [CrossRef]
12. Huang, C.; Wang, L.; Zhang, Z.; Yeung, R.S.C.; Bensoussan, A.; Chung, H.S.H. A novel spline model guided maximum power point tracking method for photovoltaic systems. *IEEE Trans. Sustain. Energy* **2019**, *11*, 1309–1322. [CrossRef]
13. Ram, J.P.; Pillai, D.S.; Rajasekar, N.; Strachan, S.M. Detection and identification of global maximum power point operation in solar PV applications using a hybrid ELPSO-P&O tracking technique. *IEEE J. Emerg. Sel. Top. Power Electron.* **2019**, *8*, 1361–1374.
14. Obukhov, S.; Ibrahim, A.; Diab, A.A.Z.; Al-Sumaiti, A.S.; Aboelsaud, R. Optimal performance of dynamic particle swarm optimization based maximum power trackers for stand-alone PV system under partial shading conditions. *IEEE Access* **2020**, *8*, 20770–20785. [CrossRef]
15. Kermadi, M.; Salam, Z.; Ahmed, J.; Berkouk, E.M. An effective hybrid maximum power point tracker of photovoltaic arrays for complex partial shading conditions. *IEEE Trans. Ind. Electron.* **2018**, *66*, 6990–7000. [CrossRef]
16. Li, X.; Wen, H.; Chu, G.; Hu, Y.; Jiang, L. A novel power-increment based GMPPT algorithm for PV arrays under partial shading conditions. *Solar Energy* **2018**, *169*, 353–361. [CrossRef]
17. Ahmed, J.; Salam, Z. An enhanced adaptive P&O MPPT for fast and efficient tracking under varying environmental conditions. *IEEE Trans. Sustain. Energy* **2018**, *9*, 1487–1496.
18. Alik, R.; Jusoh, A. An enhanced P&O checking algorithm MPPT for high tracking efficiency of partially shaded PV module. *Solar Energy* **2018**, *163*, 570–580.
19. Mohanty, S.; Subudhi, B.; Ray, P.K. A grey wolf-assisted perturb & observe MPPT algorithm for a PV system. *IEEE Trans. Energy Convers.* **2016**, *32*, 340–347.
20. Kumar, N.; Hussain, I.; Singh, B.; Panigrahi, B.K. MPPT in dynamic condition of partially shaded PV system by using WODE technique. *IEEE Trans. Sustain. Energy* **2017**, *8*, 1204–1214. [CrossRef]
21. Manna, S.; Singh, D.K.; Akella, A.K.; Kotb, H.; AboRas, K.M.; Zawbaa, H.M.; Kamel, S. Design and implementation of a new adaptive MPPT controller for solar PV systems. *Energy Rep.* **2023**, *9*, 1818–1829. [CrossRef]
22. Pradhan, C.; Senapati, M.K.; Ntiakoh, N.K.; Calay, R.K. Roach Infestation Optimization MPPT Algorithm for Solar Photovoltaic System. *Electronics* **2022**, *11*, 927. [CrossRef]

23. Awan, M.M.A.; Javed, M.Y.; Asghar, A.B.; Ejsmont, K. Performance optimization of a ten check MPPT algorithm for an off-grid solar photovoltaic system. *Energies* **2022**, *15*, 2104. [CrossRef]
24. Elkholy, M.M.; Fathy, A. Optimization of a PV fed water pumping system without storage based on teaching-learning-based optimization algorithm and artificial neural network. *Solar Energy* **2016**, *139*, 199–212. [CrossRef]
25. Palaniswamy, A.M.; Srinivasan, K. Takagi-Sugeno fuzzy approach for power optimization in standalone photovoltaic systems. *Solar Energy* **2016**, *139*, 213–220. [CrossRef]
26. Abdel-Salam, M.; El-Mohandes, M.T.; Goda, M. An improved perturb-and-observe based MPPT method for PV systems under varying irradiation levels. *Sol. Energy* **2018**, *171*, 547–561. [CrossRef]
27. Yan, K.; Du, Y.; Ren, Z. MPPT perturbation optimization of photovoltaic power systems based on solar irradiance data classification. *IEEE Trans. Sustain. Energy* **2018**, *10*, 514–521. [CrossRef]
28. Ibrahim, A.W.; Shafik, M.B.; Ding, M.; Sarhan, M.A.; Fang, Z.; Alareqi, A.G.; Al-Rassas, A.M. PV maximum power-point tracking using modified particle swarm optimization under partial shading conditions. *Chin. J. Electr. Eng.* **2020**, *6*, 106–121. [CrossRef]
29. Kaya, C.B.; Kaya, E.; Gokkus, G. Training Neuro-Fuzzy by Using Meta-Heuristic Algorithms for MPPT. *Comput. Syst. Sci. Eng.* **2023**, *45*, 69–84. [CrossRef]
30. Zafar, M.H.; Khan, N.M.; Mirza, A.F.; Mansoor, M.; Akhtar, N.; Qadir, M.U.; Moosavi, S.K.R. A novel meta-heuristic optimization algorithm based MPPT control technique for PV systems under complex partial shading condition. *Sustain. Energy Technol. Assess.* **2021**, *47*, 101367.
31. Ali, E.M.; Abdelsalam, A.K.; Youssef, K.H.; Hossam-Eldin, A.A. An enhanced cuckoo search algorithm fitting for photovoltaic systems' global maximum power point tracking under partial shading conditions. *Energies* **2021**, *14*, 7210. [CrossRef]
32. Chekired, F.; Larbes, C.; Rekioua, D.; Haddad, F. Implementation of a MPPT fuzzy controller for photovoltaic systems on FPGA circuit. *Energy Procedia* **2011**, *6*, 541–549. [CrossRef]
33. Singh, N.; Gupta, K.K.; Jain, S.K.; Dewangan, N.K.; Bhatnagar, P. A flying squirrel search optimization for MPPT under partial shaded photovoltaic system. *IEEE J. Emerg. Sel. Top. Power Electron.* **2020**, *9*, 4963–4978. [CrossRef]
34. Ahmed, J.; Salam, Z. A Maximum Power Point Tracking (MPPT) for PV system using Cuckoo Search with partial shading capability. *Appl. Energy* **2014**, *119*, 118–130. [CrossRef]
35. Mohanty, S.; Subudhi, B.; Ray, P.K. A new MPPT design using grey wolf optimization technique for photovoltaic system under partial shading conditions. *IEEE Trans. Sustain. Energy* **2015**, *7*, 181–188. [CrossRef]
36. Alam, D.F.; Yousri, D.A.; Eteiba, M.B. Flower pollination algorithm based solar PV parameter estimation. *Energy Convers. Manag.* **2015**, *101*, 410–422. [CrossRef]
37. Hadji, S.; Gaubert, J.P.; Krim, F. Real-time genetic algorithms-based MPPT: Study and comparison (theoretical an experimental) with conventional methods. *Energies* **2018**, *11*, 459. [CrossRef]
38. Al-Majidi, S.D.; Abbod, M.F.; Al-Raweshidy, H.S. A particle swarm optimisation-trained feedforward neural network for predicting the maximum power point of a photovoltaic array. *Eng. Appl. Artif. Intell.* **2020**, *92*, 103688. [CrossRef]